

Lawrence Berkeley National Laboratory

Lawrence Berkeley National Laboratory

Title

ONE DIMENSIONAL-TWO PHASE PARTICULATE FLOW

Permalink

<https://escholarship.org/uc/item/3sk8w59p>

Author

Kleist, D.M.

Publication Date

1977-09-01

00004905173

UC-25
LBL-6967
e1

ONE DIMENSIONAL-TWO PHASE PARTICULATE FLOW

Daniel Mathias Kleist
(M. S. thesis)

September 1977

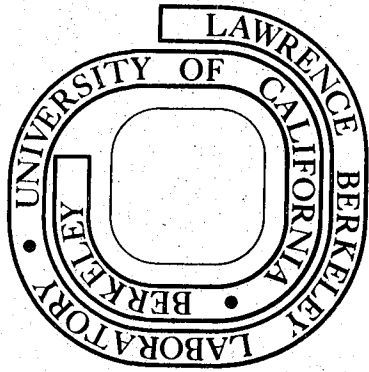
RECEIVED
LAWRENCE
BERKELEY LABORATORY

JAN 27 1978

LIBRARY AND
DOCUMENTS SECTION

Prepared for the U. S. Department of Energy
under Contract W-7405-ENG-48

For Reference
Not to be taken from this room



LBL-6967
c1

LEGAL NOTICE

This report was prepared as an account of work sponsored by the United States Government. Neither the United States nor the Department of Energy, nor any of their employees, nor any of their contractors, subcontractors, or their employees, makes any warranty, express or implied, or assumes any legal liability or responsibility for the accuracy, completeness or usefulness of any information, apparatus, product or process disclosed, or represents that its use would not infringe privately owned rights.

TABLE OF CONTENTS

ABSTRACT	vi
ACKNOWLEDGMENT	vii
I. INTRODUCTION	1
Significance of Solid Particle Velocity Prediction in Erosion Research.	1
Literature Survey	2
Scope of Present Study	4
II. THE COMPUTER MODEL	6
Introduction	6
Type of Modeling	6
Assumptions	6
Solution Technique	7
III. PROGRAM MODIFICATIONS	9
Introduction	9
Modifications to Generalize Program	10
Modifications to Improve Accuracy	11
Modifications to Expand Limits of Computation.	14
Modifications Considered but Deemed Insignificant	17
IV. ADDITIONAL ANALYSIS	20
Introduction	20
Initial Particle Velocity	20
Particle Concentration	21
V. EXPERIMENTAL DETAILS	23
Introduction	23
Description of Experimental Blast Tester	23

Determination of Computer Input Data	23
Measurement of Loading Factor	24
Measurement of Exit Particle Velocity.	27
VI. EXPERIMENTAL RESULTS	32
Introduction	32
Description of Particles	32
Loading Factor Measurements	33
Results of Particle Exit Velocity Measurements	36
VII. COMPARISON OF THEORETICAL AND EXPERIMENTAL RESULTS	42
Introduction	42
Program Predictions of Particle Exit Velocity	42
Comparison of Theoretical and Experimental Results.	43
Variation of Particle Velocities Due to Major Particle Parameters	47
VIII. CONCLUSIONS AND RECOMMENDATIONS FOR FURTHER RESEARCH	50
Use of Verified Computer Program in Place of Experimental Measurements	50
Current Use of Program.	50
Recommendations for Further Research	51
REFERENCES	52
FIGURES	54
APPENDICES	69
Basic Equations Utilized by Crowe	69
Nomenclature for Basic Program	72
Crowe's Basic Program: Gas Only	74
Crowe's Basic Program: Gas-Particle Flow.	75
Nomenclature for Modified Program	77

Modified Program Listing: English Units	81
Modified Program Listing: S.I. Units.	84

ONE DIMENSIONAL-TWO PHASE PARTICULATE FLOW

Daniel Mathias Kleist
(M.S. Thesis)

Materials and Molecular Research Division, Lawrence Berkeley
Laboratory and Department of Mechanical Engineering; University
of California, Berkeley, California

September 1977

ABSTRACT

A computer model, originally developed by Crowe at Washington State University, which predicts the velocity of solid particles entrained in a one-dimensional gas stream, is modified to improve its accuracy and extend the range of velocity prediction. The program is also used to demonstrate the effects that initial particle velocity and particle concentration have on velocity predictions. The accuracy of the model is confirmed by comparing the theoretical predictions with experimentally measured velocities of particles varying in size, shape and density. For all cases where test data could be measured accurately, the theoretical predictions are shown to be in good agreement with the average experimental values.

ACKNOWLEDGMENTS

Special thanks are extended to Professor Clayton Crowe of Washington State University for the use of his computer model and the helpful suggestions offered during the modification of the program.

I am grateful to Professor Iain Finnie for his guidance and understanding during the course of this study. Thanks are also due to Professors Lawrence Talbot and Earl R. Parker for reviewing the manuscript and to Mr. A. Levy who organized the overall research program on erosion of which this work is a part.

The assistance of Mr. Walter Toutolmin with the refurbishment of the test apparatus and the construction of the rotary disk particle velocity measurement equipment and especially his dedication to perfection is greatly acknowledged.

I am also indebted to my wife, Gudrun for her patience and understanding during the extensive time period involved in preparing the manuscript.

This work was done under the auspices of the U. S. Energy Research and Development Administration.



I. INTRODUCTION

Significance of Solid Particle Velocity Prediction in Erosion Research

The problem of erosion caused by solid particles in a gas stream is of great importance in industrial, naval and aeronautical applications. The operation of gas turbine powered vehicles and helicopters in desert areas or other solid particle polluted atmospheres, for example, has led to severe erosion problems. Solid particles can also lead to erosion causing losses in efficiency and a decrease in life in such units as coal turbines and coal gasification plants.

The importance of coal energy conversion technology in our overall energy picture requires that the mechanisms of erosion be thoroughly investigated in order to establish component design guides and material design criteria for the development of more economically efficient alloys and refractories. This was the primary motivation for the present work.

The process of erosion is a function of several variables. Early experimenters expressed the amount of erosion as a function of fluid pressure or fluid velocity. Finnie¹ suggests that an understanding of erosion may be divided into two major parts. The first part involves a determination of the number, direction and velocity of the impinging particles from the fluid flow conditions. With this information available, the second part of the problem is a calculation of the amount of surface material removed. Others² have added the temperature of the gas and eroding particles as parameters to be considered.

Erosion occurs when particles are projected against a target causing surface damage and removal of material. The amount of erosion incurred

is dependent upon the angle at which the particles strike the surface and their velocity. The velocity and direction of an abrasive particle in a fluid, however, are not necessarily the same as those of the fluid. In most erosion testers, for example, the particles travel a fairly short distance in the high velocity gas before reaching the specimen and their velocity will thus be only a fraction of the gas velocity. This uncertainty in the particle velocity makes it impossible to correlate the results of different experimenters if only the fluid velocity is reported. For this reason, many^{1,2,3,4} recent analytical predictions of erosion damage are expressed as a function of the particle velocity and its angle of impact.

The angle of particle impact can be regulated experimentally⁵ by placing a flat specimen at a predetermined angle directly below a one-dimensional nozzle of a blast tester. However, the determination of particle velocity, or more importantly, its accurate regulation for use in erosion research is not so easily achieved.

Literature Survey

Several experimental techniques have been used by researchers to measure particle velocities. The most common methods utilized are photographic techniques. Examples are: high speed photography,⁶ which produces streak photographs of single particles; double-flash exposure,^{1,5,7} which produces photographs of single particles in two positions; and high speed cinematography,⁸ in which several thousand frames per second are taken. Each of these techniques has the ability to measure fairly accurately the particle velocity, as distinct from the fluid velocity, but all are extremely time consuming and can become

quite expensive. Moreover, these methods measure the particle velocities for only one set of particle and flow parameters. When a new condition is imposed, the method must be repeated.

Due to the difficulty in physically measuring particle velocities, many^{3,4,9,10} researchers have either assumed that the particles are moving at the same velocity as the gas or have created conditions such that this assumption is valid by using small particles ($< 100\mu$) and increasing the distance in which the particles are accelerated toward the fluid velocity.

The analysis of gas-particle flow is complicated by the fact that not only must the conservation equations account for the mass, momentum and energy of each phase, but additional equations are required which relate the mass, momentum and energy transfer (coupling) between phases. The problem becomes quite complex due to the fact that the coupling equations involve several parameters such as particle size and density, local pressure and temperature, etc.

Due to this complexity and the fact that this problem is basically one of fluid mechanics, erosion researchers interested in correlating fundamental mechanisms of erosion with particle velocities^{1,5,6,9} have previously relied on experimental techniques for accurate velocity measurement or simply applied Newton's second law of motion to estimate particle velocities, by assuming Stokes' Law is valid and that the aerodynamic drag is responsible for particle motion.

More rigorous analyses of one-dimensional gas-particle flows have recently appeared in the literature incorporating particle-gas coupling. Kliegel,¹¹ for example, has successfully applied this technique to

predict performance losses in rocket nozzles. Also, Tabakoff and Hussein² applied a similar technique to study gas-particle flow through a cascade. These studies, however, were performed for specific applications and therefore do not specifically solve for particle velocities. Moreover, the analysis is mostly theoretical and cannot be easily adapted to solve for particle velocities in a typical erosion tester.

Scope of Present Study

The objective of this study is to develop an analytical computer model of a gas-particle flow system which can consistently predict, within experimental accuracy, the exit velocity of solid particles entrained in a one-dimensional gas stream. The main purpose of this program is to give erosion researchers an easy and efficient method of controlling particle velocities, over a wide range of operating conditions, as a function of the differential pressure across the nozzle of an erosion tester.

A computer program for two-phase flow, incorporating the mutual momentum exchange between phases, has recently been developed by Crowe¹² at Washington State University. This program is used as a starting point and, with appropriate modifications, is adapted to meet the objectives of this study.

The basic program is first modified to accept input data which describes the physical parameters of the test apparatus and establishes the particle and gas properties being used.

The program is then further modified to improve its accuracy by expanding parameters, expressed as constants, to variables utilizing input data and other program variables. Several additional modifications

are investigated, analyzed and adapted to further improve the accuracy and extend the limits of computation or rejected when deemed insignificant.

Additional analysis is also presented to investigate the effect of initial particle velocity and particle concentration on the exit particle velocity.

An erosion test device, originally developed by Sheldon⁵ is used to feed particles into a gas stream which accelerates the particles down the length of a small diameter tube as a function of an imposed pressure differential.

The exit velocities of steel shot, glass spheres and silicon carbide particles ranging in size from 160 μ to 660 μ are measured, using a dual flash photographic technique and a rotary disk technique which will be described later, at several selected pressure differentials between 0-15 psi. The particle concentration is also measured, for use as input to the computer program, for all conditions in which velocity measurements were made.

The exact conditions under which each velocity measurement was made is the input for the computer program and the results of the theoretical particle velocity predictions are plotted as a function of differential pressure. The results of the experimental measurements are then plotted on the same graph to illustrate the accuracy of the theoretical predictions. Additional comparisons are also presented which demonstrate the effect of particle size and density and the effect of particle concentrations on the particle exit velocity.

II. THE COMPUTER MODEL

Introduction

A brief description of the type of modeling, the assumptions, and the method of solution used in the basic computer program adapted for this study, is presented here for background information. The computer model, developed by Crowe¹² at Washington State University, is listed in the Appendix in its original form.

Type of Modeling

This model, of a one-dimensional gas-particle flow system, was developed using the conservative variable approach. The conservation equations not only account for the mass, momentum and energy of each phase, but additional equations are also incorporated to relate the mass, momentum and energy transfer (coupling) between phases.

These coupling equations incorporate the equation of state, convective heat transfer between particles and gas, wall friction, particle-gas mass flow ratio, particle trajectory, aerodynamic drag on the particle due to its relative motion with respect to the gas and several other parameters, such as particle size and density, local pressure and temperature, etc. A summary of the basic equations used by Crow, his original computer program and the modified program are given in the Appendix.

Assumptions

The following assumptions for gas-particle flow were utilized in the derivation of the governing equations: 1) The flow is one-dimensional and steady state; 2) the flow rates of both the gas phase and particles are considered constant; 3) there are no mass or energy

losses from the system; 4) there is no mass exchange between the phases; 5) the volume occupied by the particles is negligible; 6) the particles do not interact; 7) the gas is a perfect gas of constant composition; 8) the particle size is approximated by spheres of uniform diameter; 9) the particles are incompressible and have uniform properties; 10) the specific heat of the particles remains constant; 11) the internal temperature of the particles is uniform and; 12) the heat transfer between the gas and the particles is by convection only, and is basically due to their mean temperature difference. These assumptions are reasonable for most gas-particle flow in nozzles.

Solution Technique

The equations of gas-particle flow are solved using an iterative solution technique. The step by step numerical solution is derived by dividing the distance along the nozzle into a number of small increments (cells) and formulating finite difference equations.

The program is written to determine the final conditions, given appropriate initial (inlet) conditions along with the prescribed exit pressure of the gas. The inlet pressure and temperature of the gas and the initial temperature and velocity of the particles are all prescribed. An initial value of the gas velocity is guessed and used to evaluate the momentum and energy terms in the first cell.* Then, by means of the

* This solution technique was developed by Crowe and presented in his notes (ref. 12) but was not included in his original program listing in the Appendix. He simply incorporates the "correct" initial gas velocity in the program variables X, Y, & Z.

finite difference equations, the solution is carried out successively down the nozzle by using the results computed in the previous cell to obtain new results for the new cell. This procedure is repeated until the exit cell is reached, where a comparison is made between the given exit pressure and the calculated pressure. If the calculated pressure is greater than (or less than) the prescribed pressure, the guess of the initial gas velocity is increased (or decreased) and the iterative calculation scheme is repeated. When the difference between the calculated and the prescribed exit pressures is less than a designated tolerance, the computation is ended and the results at the nozzle exit are printed out.

III. PROGRAM MODIFICATIONS

Introduction

The first objective of this study is to develop a computer program designed to give erosion researchers an easy and efficient method of controlling particle velocities over a wide range of operating conditions. The basic computer model, developed by Crowe (see Section II), is used as a starting point and, with appropriate modifications, is adapted to meet this objective.

The computer model developed by Crowe incorporates many of the most sophisticated techniques known to date to model one-dimensional gas-particle flow. Although the basic computer program (listed in the Appendix) incorporates these techniques, it relies on empirically determined input data which is valid only within the limits of the particular conditions to be investigated. This requires the user to have a good estimation of the results to be obtained before using the program, in order to determine the range of such parameters as the flow and particle Reynolds numbers and the temperature of the gas, etc. Using these estimations, the user must then hand compute several parameters and input these as constants to the program.

In order to adapt the program to meet the objectives of this study, modifications are implemented to produce a more general program which only requires input to describe the test apparatus, the appropriate gas and particle properties and initial conditions. Then, utilizing this physical data the program internally computes the instantaneous fluid-mechanic parameters in each cell and continually updates these parameters

for use in expressions which are expanded as functions of these "current" values. These modifications not only make the program more general in scope and therefore more user oriented, they also improve the accuracy of computation by using the results of instantaneous parameters in place of constant approximations.

Several additional modifications are investigated, analyzed and adapted to further improve the accuracy and extend the limits of computation, or rejected when deemed insignificant.

Modifications to Generalize Program

To generalize the program, parameters expressed as constants in the basic program, which establish the initial mass, momentum and energy conditions of the gas, are expanded into terms utilizing input data and information contained within the program. The expanded variables are:

$$x = \rho u$$

$$y = p g_c + x u$$

$$z = x[u^2/2 + \gamma p g_c / \rho(\gamma-1)].$$

Where: u = initial gas velocity

ρ = initial gas density

p = initial gas pressure

g_c = constant of proportionality in Newton's 2nd Law

γ = specific heat ratio of the gas.

The necessary information contained within the program is:

(1) the initial gas velocity, which is guessed and modified as appropriate (see Section II); (2) the constant of proportionality (g_c) which is $32.174 \text{ lb}_m\text{-ft/lb}_f\text{-sec}^2$ or 1 kg-m/N-sec^2 and; (3) the specific heat ratio (γ) and gas constant (R) which are established by the choice of gas to be used.

The input data necessary to compute these parameters are simply the initial pressure and temperature of the gas, which immediately establishes p and are used with the gas constant R to establish ρ .

These expressions were used by Crowe as dependent variables for the derivation of the statement functions VGF, DGF, PGF & TGF (see program listing in Appendix).

Modifications to Improve Accuracy

The viscosity and thermal conductivity of any gas is extremely temperature sensitive. To enable this program to predict conditions accurately over a range of gas temperatures, analytical expressions for the dynamic viscosity and thermal conductivity of the gas are generated as a function of its absolute temperature. The gas used throughout this study is air, however the following discussion can be applied to any perfect gas.

If a functional relation between two variables is not logarithmic (or exponential) it can usually be analytically modeled as an interpolating polynomial in the form:

$$y = a_1 + a_2x + a_3x^2 + \dots + a_{n+1}x^n.$$

A good approximation of the dynamic viscosity (μ) and thermal conductivity (k) of air in the range of absolute temperatures (T) of 460-1800°R (256-1000°K) can be generated for $n = 2$ in the above equation. Using tabulated values of these properties at temperatures spaced throughout the temperature range, a set of three equations with three unknowns can be written in the form:

$$y_1 = a_1 + a_2 x_1 + a_3 x_1^2$$

$$y_2 = a_1 + a_2 x_2 + a_3 x_2^2$$

$$y_3 = a_1 + a_2 x_3 + a_3 x_3^2.$$

Applying the tabulated data to the above equations, with $y = k$ or μ and $x = T$, the numerical values of a_1, a_2 & a_3 can be calculated. The results, computed for air as a function of the temperature in $^{\circ}\text{R}$ and utilized in the program, are as follows:

$$\mu = [3.614\text{E-}02 + (1.753 \text{E-}04)T - (2.176 \text{E-}08)T^2]10^{-4} \text{ lb}_m/\text{sec-ft}$$

$$k = 1.258\text{E-}03 + (2.785\text{E-}05)T - (3.813 \text{E-}09)T^2 \text{ Btu/hr-ft-}^{\circ}\text{R}.$$

The Nusselt number (Nu) and the D'arcy-Weisbach friction factor (f) are used to determine the heat transfer and shear stress respectively, between the gas and the nozzle wall. Both of these expressions are functions of the flow Reynolds number (Re). Due to the large range of Reynolds numbers encountered in the computation of this program, an expression for Re was added along with the functional relations $\text{Nu} = f(\text{Re})$ and $f = g(\text{Re})$.

The flow Reynolds number is defined as:

$$\text{Re} = \rho V_g D / \mu.$$

Where: ρ = current density of gas

V_g = current velocity of gas

D = characteristic dimension (diameter of nozzle)

μ = current dynamic viscosity of gas.

An acceptable relation for $Nu = f(Re)$ for turbulent flow of gases inside smooth tubes can be expressed as:

$$Nu = 0.023Re^{0.8}.$$

A convenient relation for $f = g(Re)$ for turbulent flow inside smooth tubes is:

$$y = ax^b.$$

This power curve can be written as: $\ln y = b \ln x + \ln a$ and solved as a linear regression problem. Given the data pairs $\{(x_i, y_i), i = 1, n\}$ the coefficients a and b can be determined as follows:

$$b = \frac{\sum \ln x_i \cdot \ln y_i - (\sum \ln x_i \cdot \sum \ln y_i) / n}{\sum (\ln x_i)^2 - (\sum \ln x_i)^2 / n}$$

$$a = \exp[\sum (\ln y_i) / n - b(\sum \ln x_i) / n].$$

Choosing n -data pairs (Re_i, f_i) from the Moody diagram for smooth tubes and inserting the results in the above equations, the coefficients a and b can be determined. The results produced and utilized in the program are as follows:

$$f = 3.051 E-01 Re^{-2.463 E-01}.$$

Only one expression for the coefficient of drag (C_D) on the particles is included in the basic program:

$$C_D = 24(1 + 0.15Re_p^{0.687}) / Re_p.$$

Where: Re_p = particle Reynolds number

$$= \rho d_p |(u_g - u_p)| / \mu$$

and: ρ = current density of gas

d_p = diameter of particle

$|(u_g - u_p)|$ = absolute velocity difference between gas and particles

μ = current dynamic viscosity of gas.

This expression for C_D corresponds fairly well with experimental values for spherical particles, up to $Re_p = 700$. The particle Reynolds numbers typically encountered during computation, however can be much greater than 700.

Several empirically determined expressions for C_D have been compiled by Boothroyd.¹⁶ Comparing these expressions with experimentally determined drag coefficients at various particle Reynolds numbers, the following expressions for $C_D(Re_p)$ are adapted for use in the program, over the range of Re_p indicated:

$$C_D = 24(1 + 0.15Re_p^{0.687})/Re_p \quad (0 < Re_p < 200)$$

$$C_D = 21.9416Re_p^{-0.718} + 0.324 \quad (200 \leq Re_p < 2500)$$

$$C_D = 0.4 \quad (Re_p \geq 2500).$$

Each the above modifications successfully replaced the constant or limited expressions used in the basic program, producing a more accurate computer program.

Modifications to Expand Limits of Computation

With the modifications to improve the accuracy complete, the computer program was run, using wide ranges of particle parameters and operating conditions, to check the stability of the program. For most conditions tested, the program remained stable and produced reasonable results. Two extreme conditions however, caused the program to become unstable.

When very small, low density particles [Coal Char: $\sim 100 \mu\text{m}$; $60 \text{ lb}_m/\text{ft}^3$ (0.96 gm/cm^3)] were used in the program, it became unstable. This instability occurred when the calculated velocity of the particles, V_p , exceeded that of the gas, V_g . Since the particles are dribbled into the high velocity gas stream and accelerated by the gas, this condition could never occur naturally.

A check was added to the program which set the particle velocity equal to the gas velocity when V_p first exceeded V_g and then printed out all of the results in each cell. The results from this check, using 50 cells for a 24 inch nozzle, showed this condition occurred in the first cell. The length of each cell, for this example, was 24 in/ 50 cells or 0.48 in/cell, which greatly exceeds the concept of differential increments, dx . This situation was later determined to be the source of the instability.

To verify this conclusion, the number of cells was increased to 200 (0.12 in/cell). This allowed the previous example to run with no instabilities, however when still smaller particles were used, the same instability occurred. An increase to 400 cells (0.06 in/cell) produced a program which was stable for all particles of interest.

When large pressure differentials across the nozzle ($\Delta P > 25\text{psi}$) were tried in the program, it again became unstable. This condition occurred when the velocity of the gas exceeded the local speed of sound. The velocity of a gas in a one-dimensional nozzle, however, can never exceed sonic conditions. When this impossible situation occurred during the computation, the argument (ARG) of the square root term in the statement function VGF became negative.

A check was added to the program which set the initial guess of gas velocity to a lower value when ARG became negative. This allowed the program to run at somewhat larger ΔP 's without instability, by keeping the initial gas velocity guess low enough, so as not to exceed sonic conditions during the iteration to find the initial gas velocity. When large enough ΔP 's were used which caused the exit velocity to become sonic, no matter what initial V_g was guessed, an infinite loop resulted.

In a one-dimensional nozzle, when the back pressure (exit pressure) of the flow is high enough (ΔP low enough), the flow will adjust itself, so that the exit pressure of the flow matches the back pressure and the flow is everywhere subsonic. This is the condition used in the iteration scheme to find the initial V_g . As the back pressure becomes lower (larger ΔP), the flow velocity increases more, until the back pressure is low enough to cause the exit flow velocity to become sonic. The nozzle is then choked. Further decreases of the back pressure (even larger ΔP) no longer effect the flow upstream and the exit pressure is greater than the back pressure.

With this fact in mind, a change was added to the program which allowed the check at the exit of the nozzle to be governed by the sonic speed of the gas, instead of comparing the exit pressure in the iteration scheme, producing an exit pressure greater than the back pressure. This change allowed the program to be run at any pressure differential without instability.

Due to the high velocities that could now be achieved, a suggestion from Crowe to account for Mach number effects,¹⁷ due to the relative

velocity between the particles and gas, was adopted. This involves multiplying the drag force factor by the term:

$$C = 1.65 + 0.65 \tanh(2 \ln M) + 0.425 \exp[-2.5(\ln M/\gamma)^2].$$

Where: γ = specific heat ratio of gas

$$M = |u_g - u_p|/a$$

and: $|u_g - u_p|$ = absolute velocity difference between gas and particles

a = local speed of sound.

Modifications Considered but Deemed Insignificant

The program assumes that the particles are spherical in shape. Irregular shaped particles, such as silicon carbide, have a greater surface area per unit volume than for spheres of the same volume. For this reason, techniques were investigated to determine an equivalent spherical diameter for irregular shaped particles.

Two techniques were used to determine this equivalent diameter, using +100-80 mesh silicon carbide particles. (1) With the aid of a microscope, 100 particles were counted and placed in a container. These particles were weighed to determine the average weight of each particle. Then, dividing this weight by the particle density, the average volume of each particle was determined. A diameter corresponding to this volume, taken as a sphere, was determined. (2) Another method was used to determine the equivalent diameter by measuring the physical dimensions of several particles from an electron microscope picture to determine the average volume of each particle, and consequently its equivalent diameter.

Both of these techniques produced equivalent diameters of ~160 to 180 μm . The diameter of these particles, based on the mesh size of the

sieves, was taken to be 160 μm . The difference in particle velocities computed for 160 μm and 180 μm particles at several particle loadings, was not significant enough to warrant this additional task of determining an equivalent diameter. Much larger irregular particles ($> 500 \mu\text{m}$) however, may produce a significant error.

The program uses the actual length of the nozzle for computation. The effect of contraction from the mixing chamber into the top of the nozzle and the effect of expansion from the nozzle into the test chamber (see Figure V-1 for arrangement of test apparatus) could cause additional losses to the system. This condition was investigated by running the program and increasing the length of the nozzle slightly to produce an equivalent length which would account for such losses. Small changes in the length of the nozzle again produced insignificant differences in the particle velocities to justify the determination of the actual losses or adding a guess of an equivalent length for the losses.

It was noted in experiments performed by Sheldon⁵ that, as the nozzle eroded, the particle velocities changed significantly. To check to see if this condition could be caused by an effective increase in nozzle diameter, the program was run using 160 μm particles at constant loading factors of 0.1, 0.5 and 1 for nozzle diameters of 0.175, 0.180 & 0.185 inches. The results (all using the smooth tube friction factor equation) showed that the particle velocities changed only about 3% for any pressure differential at each loading. Therefore, increasing the effective diameter of the nozzle to account for erosion of its sides, was not justified.

The contradiction between Sheldon's observations and the program's calculations is probably due to the fact that, as the tube erodes, the wall is no longer smooth and consequently, the D'arcy-Weisbach friction factor (f) is effected. To eliminate this problem, the erosion of the nozzle was checked periodically during testing and exchanged if deemed necessary.

IV. ADDITIONAL ANALYSIS

Introduction

In addition to the modifications presented in Section III, further analysis is presented here to examine the effects of initial particle velocity and particle concentration on the particle exit velocity.

Initial Particle Velocity

The time of flight of a particle through each differential cell of the nozzle is defined as the length of the cell divided by the velocity of the particle. In terms of the program variables, this relation is expressed as:

$$DT = DX/VP(I-1). \quad (\text{Eq. IV-1})$$

Where I = the cell number.

Also, the particle velocity in each successive cell is equal to the particle velocity in the preceding cell plus a momentum source term due to the particles. This momentum source term is the product of the time of flight of particles (DT) and other terms involving the velocity difference between the gas and particles, drag force on the particles and Stoke's constant. For the purpose of this discussion, the new particle velocity can be expressed as:

$$VP(I) = VP(I-1)+DT*TERMS. \quad (\text{Eq. IV-2})$$

It can be seen from Equation IV-1 that, as the initial particle velocity (VP(1)) approaches zero, the time of flight (DT) approaches infinity. This, by Equation IV-2, causes the particle velocity in the second cell to also approach infinity. This condition causes the program to become unstable. As the initial velocity is increased, the program

becomes more stable and the exit velocity stabilizes to a value dependent on the particles used and the differential pressure imposed.

As an example, Fig. IV-1 illustrates the effect of initial particle velocity on the exit particle velocity, for 300 μm steel shot at differential pressures of 5, 10 and 15 psi. The point of stabilization is seen to be approximately 5 ft/sec over the pressure range 0-15 psi. Other examples, using different particles and sizes, were run on the computer producing similar results. Therefore, the initial particle velocity was chosen to be 5 ft/sec for all computer predictions.

Particle Concentration

A convenient parameter to express particle concentration is the loading factor, defined for this study as the particle-gas mass flow ratio. The gas flow rate is controlled by the differential pressure imposed on the nozzle. Therefore, a constant particle flow will not yield a constant loading factor or particle concentration, over a range of differential pressures. Conversely, a constant loading factor represents a variable particle loading.

Increasing the particle concentration causes a decrease in the system momentum and energy. Therefore, the particle concentration, or loading factor, effects the exit velocity of the particles. To examine this effect, a computer run was made, using 130 μm silicon carbide at constant loading factors of 0.5 and 1.0 gm/gm and over a differential pressure range of 0 - 40 psi. Figure IV-2 illustrates these program predictions.

In order to determine how much the loading factor can effect the velocity predictions, the computation illustrated is one in which the conditions are extreme. The particles are very small and light ($130 \mu\text{m}$, 3.20 gm/cm^3), the loading factors are held constant (requiring an increasing particle loading with increasing differential pressure), and the differential pressure range is run beyond the 15 psi limits of the testing equipment. These conditions illustrate the large difference in particle velocity which may result from changes in loading. In Fig. IV-2, at a differential pressure (ΔP) of 15 psi, a velocity difference of $\sim 23 \text{ m/sec}$ exists between the predictions for 0.5 and 1.0 gm/gm loading factor and, for $\Delta P = 40 \text{ psi}$, a difference of $\sim 45 \text{ m/sec}$. If the real loading factor for this particle is actually 1.0 gm/gm at $P = 15 \text{ psi}$ and an assumed loading factor of 0.5 gm/gm is used for the computer prediction, the results could be as much as 15% off or, at $P = 40 \text{ psi}$, as much as 20% off. For this reason, it was decided that the loading factor can be an important parameter for accuracy in particle velocity predictions and therefore, should be physically measured and input into the program at each pressure differential to be tested.

V. EXPERIMENTAL DETAILS

Introduction

The main objective of this experiment is to verify the accuracy of the computer predictions of the exit particle velocities. In order to achieve this objective, accurate values of all data needed as input to the program have to be determined and controlled. A blast tester device, originally used by Sheldon⁵ for his study of erosion of brittle materials, was adapted to meet this objective.

Description of Experimental Blast Tester

The basic operation of this apparatus is similar to a sand blaster, in which particles are introduced into a high velocity gas stream and accelerated through a nozzle. A sketch of the basic components of this tester is shown in figure V-1. Particles are placed in the particle hopper and are dribbled through the feed tubes into the particle and gas mixing chamber by agitating the hopper with an air actuated vibrator. Carrier gas is conveyed to the particle and gas mixing chamber from a pressure source. A pressure differential is imposed across the ends of the nozzle due to the pressure of the carrier gas in the mixing chamber at the top of the nozzle and, for subsonic flow, atmospheric pressure at the nozzle exit. This pressure differential produces gas flow through the nozzle. The particles entering the mixing chamber are accelerated, through the nozzle, by the gas flow and exit into the test chamber.

Determination of Computer Input Data

Several needed input data are established by the choice of nozzle, operating temperature, carrier gas, and particles used. The length,

diameter and roughness of the nozzle are established by using a smooth tube and physically measuring its inside diameter and length. All tests are run at room temperature, therefore the temperature of the nozzle wall and the initial temperatures of the gas and particles are taken to be approximately ambient. The properties of the carrier gas are established by using air, whose ratio of specific heats and gas constant are well known, and whose viscosity and thermal conductivity are easily generated as functions of absolute temperature. The particle diameter is determined by sifting particles through a series of sieves and published values were taken for their density and specific heat.

Other needed input data are controlled by adjusting components of the blast tester. The differential pressure, and consequently the gas flow rate, is controlled by adjusting the gas pressure in the mixing chamber and monitoring it with the nozzle pressure gage, as shown in Fig. V-1. The particle feed rate is controlled by adjusting the air pressure to the vibrator and noting its value on the vibrator pressure gage, and by adjusting the inclination of the particle feeder and noting the height Δ .

The final two input data needed are; the initial particle velocity, which is chosen to be 5 ft/sec, and; the loading factor, which has to be calculated.

Measurement of Loading Factor

The loading factor, as previously described, is the ratio of the particle and gas mass flow rates, i.e.;

$$\text{Loading} = \frac{\dot{m}_p}{\dot{m}_g}.$$

The mass flow rate of the particles, \dot{m}_p , is adjusted by varying their feed rate. At any fixed setting of vibrator pressure and hopper inclination, the particle feed rate remains constant, no matter what the pressure in the mixing chamber is. This is due to the particle hopper being sealed from the outside environment and open only to the mixing chamber. Therefore, the particle mass flow rate need only be measured once for each change in particle, its size, or hopper setting.

The particle mass flow rate is determined by weighing the particles collected in a container over a timed interval. As an example, the tabulated data for 280 μm steel shot at a vibrator pressure of 30 psig and hopper inclination of $\Delta = 1.36$ in. is shown in Table V-1.

Table V-1. Particle Mass Flow Rate Data

Cup #	Time (sec)	Measured Data		Calculated Results	
		Weight (grams) Cup & Particles	Weight (grams) Cup Only	Weight (grams) Particles Only	\dot{m}_p (gm/sec)
1	29.74	41.63	1.85	39.78	1.337
2	29.77	40.95	1.84	39.11	1.314
3	29.89	40.51	1.86	38.65	1.293
Average					1.315

The average \dot{m}_p is seen to be 1.315 gm/sec or 0.174 lb_m/min.

The gas mass flow rate, \dot{m}_g , is affected by both the pressure of the carrier gas in the mixing chamber and the flow rate of the particles. Therefore, for each condition that a constant \dot{m}_p is measured, \dot{m}_g must

also be measured, at each differential pressure for which a velocity test is to be run.

The flow rate of the gas is measured by a flow meter gage in the carrier gas line. With the particles flowing into the mixing chamber at the constant \dot{m}_p previously measured, the differential pressure, ΔP , is adjusted to each value needed for the velocity tests. At each ΔP setting, the gas flow rate is recorded from the flow meter, along with its local pressure from the flow meter pressure gage. See Fig. V-1. The measured flow rate is then corrected to the true flow rate by using a correction factor, K , to correct for local pressure.

$$\text{True flow rate} = K \times \text{meter reading}$$

where

$$K = \sqrt{\frac{P_a + 14.7}{P_c + 14.7}}$$

p_a = Actual gas pressure at entrance to meter, PSIG

P_c = Calibrated gas pressure for flow meter, PSIG
($P_c = 70$ PSIG for meter used)

The smallest reading of the flow meter used in this experiment is 3 SCFM. Therefore, tests run at a differential pressure of less than approximately 3 psi cannot be read on the meter. To approximate the gas flow rate at low ΔP 's, the true flow rates, which are calculated from the readings that can be read, are plotted on graph paper as a function of differential pressure, and linearly extrapolated as shown in Fig. V-2.

The gas mass flow rate, \dot{m}_g , is now easily calculated by multiplying the true flow rate by the density of the carrier gas at standard

temperature and pressure (70°F, 1 Atm). Air is used as the carrier gas in these experiments. The density of air at STP is: $\rho_{\text{air}} = 0.0748$ lb_m/ft³.

The loading factor (\dot{m}_p/\dot{m}_g) is now easily computed at each ΔP . As an example, the tabulated data for \dot{m}_g and the calculated loading factors for the constant \dot{m}_p used in Table V-1, are summarized in Table V-2.

Measurement of Exit Particle Velocity

After all of the necessary input data for the computer program have been obtained, the program can be run to predict the particle exit velocity. In order to verify the computer predictions, the average velocity of the particles at the exit of the nozzle must be measured. Two techniques are utilized in this study and are described below.

Photographic Technique

Figure V-3 illustrates the orientation of a dual strobe flash unit and camera with respect to the test chamber. Circler metal plates at both sides of the test chamber can be replaced with glass plates when this set-up is used. With the camera focused on the nozzle exit and while particles are being accelerated through the nozzle, the shutter release is depressed. Simultaneously, the dual strobe flash unit is activated by means of a flash synchronizer, causing two flashes which are pre-set from 5 to 100 μsec apart.

The photograph thus obtained, shows particles at two positions in time. The velocity of each particle captured on the film is then the distance each individual particle has traveled, divided by the time between flashes. An average of many such particle velocities, all measured

Table V-2. Gas Mass Flow Rate Data with Calculated Loading Factors

ΔP (psi):	1	2	3	4	6	8	10	15
Flow Meter Pressure (psig)	-----	-----	72	71	69	68	67	66
Flow Meter Reading (SCFM)	-----	-----	3.9	5.2	7.5	9.7	11.4	15.3
True Flow Rate (SCFM)	(1.3) ¹	(2.6) ¹	3.9	5.2	7.5	9.6	11.2	14.9
\dot{m}_g (lb _m /min)	0.097	0.195	0.292	0.389	0.561	0.718	0.838	1.115
Loading Factor $(\dot{m}_p/\dot{m}_g)^2$	1.79	0.89	0.60	0.45	0.31	0.24	0.21	0.16

1 Bracketed values are approximated

2 Based on $\dot{m}_p = 0.174$ lb_m/min

under the same operating conditions, is used to determine a particle exit velocity.

Although this technique is straightforward in concept, its application is both expensive and time consuming. In order to obtain a good approximation of the velocity, many individual particles must be photographed and each displacement measured. Only a few particles can be captured on each photograph, in fact a significant percentage of photographs contain no particles at all! Since each photograph taken requires completing an entire controlled test procedure, obtaining enough data to measure particle velocities under several varying conditions can indeed become very time consuming. It is for this reason that only one of the six particle velocity curves presented in this report is obtained using this technique.

Rotary Disk Technique

A time-of-flight measurement method for particle velocity has been developed by Ruff and Ives¹³ at the National Bureau of Standards. This simple mechanical configuration allows the measurement to be made under a wide range of equipment conditions. The time-of-flight of the particles is determined over a controlled path length between two rotating disks.

Figure V-4A illustrates how the apparatus for this technique is adapted for use with the blast tester used in this study. A pair of metal disks mounted on a common shaft are caused to rotate directly below the nozzle exit in the test chamber. The shaft is rotated by a D.C. motor by means of a belt drive between aluminum pulleys of equal diameter mounted on the motor and disk shafts. The speed of the motor,

and hence the disks, is controlled by a variable D.C. power supply which powers the motor. This speed is monitored by an electronic revolution counter which counts the number of times a set screw on the motor pulley passes a magnetic pickup, and digitly displays one-hundreth of this number per minute. To improve the accuracy of the read-out, ten set screws are evenly spaced on the motor pulley. Therefore, a reading of 300 represents 3000 RPM.

Particles, accelerated through the blast tester under the conditions for which their velocity is to be measured, exit the nozzle and impinge on the top disk. A single radial slit in the top disk permits some of the particles to pass through and eventually erode a mark on the lower disk. Two erosion exposures are made, one with the disks stationary and the other with the disks rotating at a known, constant velocity. Measurement of the angular displacement between these marks gives a measure of the time-of-flight of the particles as they cross the space between the disks.

The parameters used in this technique to calculate the average particle velocity are illustrated in the sketch in Fig. V-4B. The time-of-flight of a particle passing through the slit is L/V_p , where V_p is the average particle velocity. During this time, the disks will have rotated by $(L/V_p)\nu$ revolutions or $(L/V_p)2\pi\nu$ radians. This angular displacement, expressed in terms of the parameters shown in Fig. V-4B, is simply S/R radians. The average velocity of the particles is then given by the relation:

$$V_p = 2\pi RVL/S.$$

All quantities in this expression can be measured directly.

In this study, polished brass disks 0.45mm thick are attached to the top side of the bottom disk and are eroded by the particles that pass through the slit in the top disk. The erosion mark thus produced represents the velocity of all the particles passing between the two disks, with the center of the mark representing the average velocity. Unlike the photographic technique, which calculates each individual particle velocity, this rotary disk technique efficiently determines the average velocity of thousands of particles with one measurement. The center of the erosion marks, however, may not always be easily determined or accurately marked for measurement. Therefore, about three separate sets of erosion marks should be taken, for each condition to be measured, and the average of these "average" velocities used as the prediction or verification of the average particle velocity. Three sets of erosion marks can easily fit on one brass disk by rotating the bottom disk relative to the top disk until a new area is exposed under the slit. Consequently, only one brass disk is required to measure the particle velocity for each condition to be measured, saving both time and expense compared with the photographic technique.

VI. EXPERIMENTAL RESULTS

Introduction

In order to verify the accuracy of the computer program to predict the exit velocity over a wide range of particle conditions, particles are chosen which vary in density, size and shape. The apparatus and techniques described in the preceding section are then used to experimentally measure the loading factor and particle exit velocity for each group of particles under various equipment conditions.

Description of Particles

The particles used in this experiment were: Glass Spheres, Steel Shot and Silicon Carbide (SiC). The choice of these particles was dictated by availability and the fact that they present a wide range of particle density (160 - 490 lb/ft³) (2.56 - 7.85 gm/cm³). Also of interest is the fact that the Glass Spheres and Steel Shot are nearly spherical, which the modeling assumes, and the SiC particles are mostly angular in shape, which deviates from the modeling.

The size of the particles to be tested is controlled by: first, ordering particles of a specified mesh size and then, sifting these particles through a series of sieves to limit their variation in size. As an example, 60 mesh Steel Shot was ordered and sifted as follows: A set of sieves was assembled, from the finest to the coarsest in ascending order (42-48-60-65 mesh), with a collecting pan at the bottom under the finest sieve. The particles were placed on the top sieve and a solid cover was added to close the nested assembly, which was then securely attached to a mechanical sieve shaker and shaken for approximately 15 minutes. The particles which passed through the 48 mesh

sieve but did not pass through the 60 mesh sieve were saved and used for testing. The openings in these sieves are 300 μm and 250 μm respectively. The "average" diameter of these particles was then chosen to be approximately 280 μm .

The necessary particle properties are readily found in the literature. Table VI-1 summarizes the particles used in this experiment along with their size range and physical and thermal properties.

Loading Factor Measurements

Section V demonstrated how the loading factor is measured and the fact that, although the particle feed rate can be controlled and kept constant for a series of tests, the loading factor is variable, depending on the mass flow rate of the carrier gas at the pressure differential of the test in progress. Therefore, loading factor measurements are made for each change in test condition (i.e.: Type of particle, particle size and particle feed rate) at each ΔP that a velocity test is to be made. Table VI-2 summarizes the type of tests to be run and the corresponding loading factor at each ΔP setting.

These measurements are made utilizing the widest range of equipment conditions available. The maximum steady pressure obtainable in the mixing chamber (ΔP) is about 18 psi. Therefore, all tests are run from 0-15 psi. All particle loading measurements, except for test #3, are taken with the maximum particle hopper inclination (Δ) at 1.36 in (3.45 cm) and the maximum vibrator pressure of 30 psi. Test #3 is taken with a lower particle loading to investigate the effect of particle concentration on the particle velocity. This test is run with an inclination of

Table VI-1. Particle Sizes and Properties

Particle Type	Shape	Size (mesh)/(μm)	Density (gm/cm^3)/($\text{lb}_\text{m}/\text{ft}^3$)	Specific Heat Capacity ($\text{cal}/\text{gm}\cdot^\circ\text{c}$)/($\text{Btu}/\text{lb}\cdot^\circ\text{F}$)
Glass Sphere	~Spherical	+32-24/500	2.56/160	0.25/0.25
Steel Shot	~Spherical	+28-24/660	7.85/490	0.12/0.12
		+60-48/280		
Silicon Carbide	~Angular	+60-48/280	3.20/200	0.20/0.20
		+100-80/160		

Table VI-2. Loading Factors

Test #	Particle Type	Size (μm)	(gm/sec)/(lb/min)	ΔP(psi):	Loading Factor (lb _p /lb _g) or (gm _p /gm _g)							
					1	2	3	4	6	8	10	15
1	Glass Sphere	500	1.15/0.153		1.73	0.90	0.59	0.42	0.28	0.22	0.19	0.14
2	Steel Shot	280	1.31/0.174		1.79	0.89	0.60	0.45	0.31	0.24	0.21	0.16
3	Steel Shot	280	0.11/0.014		0.15	0.08	0.05	0.04	0.02	0.02	0.02	0.01
4	Steel Shot	660	2.32/0.307		3.72	1.96	1.20	0.85	0.59	0.46	0.39	0.28
5	Silicon Carbide	280	0.64/0.085		1.26	0.63	0.44	0.33	0.17	0.13	0.11	0.08
6	Silicon Carbide	160	0.33/0.044		0.54	0.26	0.17	0.13	0.08	0.06	0.05	0.04

000049000193

$\Delta = 1.13$ in (2.87 cm) and a vibrator pressure of 20 psi. Lower settings of inclination and/or vibrator pressure produces an unsteady particle flow.

Results of Particle Exit Velocity Measurements

Two techniques are used to measure the particle exit velocities: (1) Photographic and (2) Rotary Disk. Due to the realitive ease of measurement using the Rotary Disk technique as compared with the photographic technique, only the first test, using Glass Spheres, is measured using the latter.

Photographic Technique

The velocity of Glass Spheres, run at the equipment settings at which their loading factors were determined, is measured using the Photographic technique. Several photographs are taken until at least five clear sets of particles are captured on film for measurement. For the velocity range encountered here, a delay between flashes, t , of 35 to 60 μ sec produces particle displacements, d , of about 3.5 to 6.5 mm. The magnification of the photograph, m , is determined by measuring the actual outside diameter of the nozzle exit and comparing it to its image in the photograph. The velocity of the particles, V_p , can then be determined by the relation:

$$V_p = d/tm. \quad (\text{Eq. VI-1})$$

As an example, Table VI-3 lists the measurements and velocities obtained at $\Delta P = 6$ psi. Results of the velocity calculations at the remaining differential pressures are shown in Table VI-5.

Table VI-3. Example of Photographic Technique Measurements

Magnification, m = 2.081						
Photo #	Particle #	ΔP (psi)	Displacement, d (mm)	Flash Delay, t (μ sec)	Velocity, V_p (m/sec)/(ft/sec)	
1	1	6	5.8	50	55.74/182.88	
	2	6	5.9	50	56.70/186.04	
2	1	6	5.9	50	56.70/186.04	
	2	6	5.9	50	56.70/186.04	
	3	6	6.2	50	59.59/195.49	
3	1	6	5.3	45	56.60/185.68	
	2	6	5.5	45	58.73/192.69	
Average					57.25/187.84	

00004903194

Rotary Disk Technique

The remaining velocity tests using Steel Shot and Silicon Carbide particles are made using the Rotary Disk Technique, at each combination of equipment settings that their loading factors were determined. The average particle velocities can be determined by use of Equation V-3:

$$V_p = 2\pi RVL/S.$$

All quantities in this expression can be measured directly. First, the distance L between the disks is set by relative placement of the two disks on the shaft. Then, with the slit in the top disk directly aligned beneath the nozzle exit, particles accelerated by a $\Delta P = 10$ psi pass through the slit for approximately 10 sec and erode an index mark on the brass disk below. Now, with disks rotating at a constant known velocity, particles accelerated by the ΔP at which the test is to be made, exit the nozzle and impinge on the top disk. Some of these particles pass through the slit and erode a second mark on the brass disk. This procedure is repeated two more times on the same brass disk producing three pairs of erosion marks to measure one velocity condition.

The brass disk is then removed from the test chamber and radial lines are scribed through the "center" of each erosion mark. An arc is then scribed between each pair of radial lines at an arbitrary distance R from the center of the disk. The lengths R and S are then measured as shown in Fig. V-4B.

As an example, Table VI-4 lists the measurements and velocities obtained for 280 μm Steel Shot at the loading conditions for test #2 and $\Delta P = 4$ psi.

Table VI-4. Example of Rotary Disk Technique Measurements

ΔP (psi)	Trial #	Angular Velocity, ω (RPM)/(RPS)	Disk Separation, L (mm)/(in)	Radial Distance, R (mm)/(in)	Arc Length, S (mm)/(in)	Velocity, V_p (m/sec)/(ft/sec)
4	1	3000/50.00	28.58/1.125	15.37/0.605	3.51/0.138	39.36/129.12
	2	3000/50.00	28.58/1.125	15.77/0.621	3.61/0.142	39.26/128.80
	3	3000/50.00	28.58/1.125	14.48/0.570	3.30/0.130	39.36/129.14
					Average	39.33/129.02

000004903195

A complete listing of all experimental velocity tests is summarized in Table VI-5.

Table VI-5. Complete List of All Experimental Particle Velocity Results

Test #	Particle Type	Size (μm)	Particle Velocity, V_p (m/sec)/(ft/sec)								
			ΔP (psi):	1	2	3	4	6	8	10	15
1	Glass Sphere	500	22.71	32.03	39.17	46.32	57.25	65.35	72.31	81.96	
			74.51	105.09	128.51	151.98	187.84	214.41	237.24	268.89	
2	Steel Shot	280	18.01	27.80	33.36	39.33	47.16	53.43	56.93	66.82	
			59.10	91.22	109.44	129.02	154.74	175.30	186.78	219.24	
3	Steel Shot	280	19.97	30.26	35.76	41.49	48.62	55.33	59.86	69.97	
			65.51	99.27	117.31	136.12	159.53	181.53	196.40	229.57	
4	Steel Shot	660	10.74	17.28	21.72	25.57	32.03	36.55	40.82	47.02	
			35.23	56.70	71.26	83.88	105.07	119.92	133.92	154.26	
5	Silicon Carbide	280	24.69	36.59	48.07	54.66	66.14	73.76	80.80	92.49	
			81.00	120.05	157.70	179.34	217.00	242.01	265.10	303.45	
6	Silicon Carbide	160	28.87	44.38	57.04	66.37	82.65	91.17	99.20	115.92	
			94.71	145.59	187.13	217.74	271.15	299.12	325.46	380.31	

00004903195

VII. COMPARISON OF THEORETICAL AND EXPERIMENTAL RESULTS

Introduction

The complete modified computer program, developed in Sections II and III, is run inputting all necessary data described in Section V along with the loading factors shown in Table VI-2. The computed particle velocity predictions, thus obtained, are tabulated and compared graphically with the results of the experimental measurements. Also, the variation in particle velocities, influenced by the major particle parameters of size, density and loading, are individually investigated.

Program Predictions of Particle Exit Velocity

The modified computer program is run inputting all necessary data in English Units. The information required by the program, necessary to describe the exact conditions of each experimental test, is submitted to the program in two ways. Part of the information is inserted into the main body of the program and the remainder is entered on data cards.

The types of information submitted internal to the program are:

- (1) Variables which are a function of computed variables (the dynamic viscosity and thermal conductivity of the gas which are functions of the current absolute temperature and the nozzle wall friction which is a function of the current flow Reynolds Number) and
- (2) Data which remains constant for all types of tests to be run (the ratio of specific heats and gas constant of the carrier gas (air) and the initial conditions of the particle temperature and particle velocity). The expressions for the variables in (1) above are derived and listed in Section III. The data used in this study for (2) above are listed below in Table VII-1.

Table VII-1. Constant Data Internal to Main Program

Program Variable	Description	Value	Units
AK	Specific Heat Ratio	1.4	----
RGAS	Gas Constant	53.35	$\frac{\text{lb}_f\text{-ft}}{\text{lb}_m\text{-}^\circ\text{R}}$
TP(1)	Initial Particle Temp	75	$^\circ\text{F}$
VP(1)	Initial Particle Velocity	5	ft/sec

The remainder of the input data is entered on data cards. Each set of data contains the information shown in Table VII-2 below. The data with numerical values remain constant for all computer runs that are to be correlated with the experimental measurements presented in Section VI. The values of these data, however, can be varied for analysis as in Section III and also for design purposes (see Section VIII). The data without numerical values vary with the type of test being examined. Their corresponding values are shown in Tables VI-1 and VI-2.

Using the input described above, the modified program is run to predict the theoretical particle velocities. The results are listed in Table VII-3.

Comparison of Theoretical and Experimental Results

The above theoretical results are compared graphically, as a function of differential pressure, with the values of the experimentally measured particle velocities listed in Table VI-5. By drawing a smooth curve through the program predictions and indicating the experimental results as separate points, as illustrated in Figs. VII-1 through VII-6,

Table VII-2. Data Card Input

Program Variable	Description	Value	Units
DPRE	Differential Pressure	See Note 1	PSI
DDL	Tube Length	12	inches
TGASF	Initial Gas Temperature	75	°F
TWF	Constant Wall Temperature	75	°f
DPM	Particle Diameter	See Note 1	microns
DIAI	Tube Diameter	0.1875	inches
FL	Loading Factor	See Note 1	$\frac{\text{lb particles}}{\text{lb gas}}$
DENP	Actual Particle Density	See Note 1	lb_m/ft^3
CCP	Specific Heat of Particle	See Note 1	$\text{Btu}/\text{lb}_m\text{-}^\circ\text{R}$

(1) Numerical values are dependent on the type and size of particles, and the loading conditions at selected values of ΔP . See Tables VI-1 and VI-2 for numerical values.

a visual comparison can be easily made.

The graphs in Figs. VII-1 through VII-5 indicate that the theoretically computed particle velocity predictions provide a good estimate of the actual (experimentally measured) particle velocities. The results illustrated in Fig. VII-6 however, show larger deviations than experienced in the other five tests.

In order to better compare these deviations, the percent difference between the theoretical and experimental results are compared, assuming the actual average particle velocity is that which was experimentally measured, and using the values listed in Tables VI-5 and VII-3. The results are shown in Table VII-4.

Table VII-3. Complete List of All Theoretical Particle Velocity Predictions

Test #	Particle Type	Size (μm)	ΔP(psi):	Particle Velocity, V _p (m/sec)/(ft/sec)							
				1	2	3	4	6	8	10	15
1	Glass Sphere	500		20.69	31.48	40.12	46.76	56.89	64.35	70.53	80.71
				67.87	103.28	131.62	153.43	186.65	211.11	231.39	264.79
2	Steel Shot	280		17.88	27.10	33.46	38.62	46.44	52.66	57.68	66.51
				58.67	88.92	109.79	126.72	152.35	172.78	189.24	218.22
3	Steel Shot	280		21.58	30.16	36.04	40.90	48.59	54.79	59.35	67.78
				70.81	98.96	118.25	134.20	159.40	179.74	194.73	222.38
4	Steel Shot	660		11.15	17.43	22.38	26.38	32.34	36.93	40.42	47.28
				36.58	57.20	73.43	86.54	106.26	121.16	132.61	155.13
5	Silicon Carbide	280		25.32	38.45	47.47	54.71	66.14	73.96	80.55	91.88
				83.09	126.15	155.73	179.48	216.99	242.65	264.27	301.46
6	Silicon Carbide	160		35.09	51.52	62.73	70.91	83.70	92.68	99.62	111.25
				115.13	169.02	205.80	232.63	274.61	304.06	326.83	364.98

00104903198

Table VII-4. Deviation of Theoretical from Experimental Particle Velocities

Test #	Particle Type	Size (μm)	ΔP(psi):	Percent Diviation (%)							
				1	2	3	4	6	8	10	15
1	Glass Sphere	500		-4	-2	+2	0	0	-2	-2	-2
2	Steel Shot	280		0	-3	0	-2	-2	-1	+1	0
3	Steel Shot	280		+8	0	0	-1	0	0	0	-3
4	Steel Shot	660		+4	0	+3	+3	0	+1	0	0
5	Silicon Carbide	280		+3	+5	-1	0	0	0	0	0
6	Silicon Carbide	160		+22	+16	+10	+7	+1	+2	0	-4

The results in Table VII-4, for tests #1 - 5, show that the percent deviation of theoretical from experimental results ranges from +8% to -4% with the majority of the deviations being between $\pm 3\%$. Note that the largest deviations occur at low pressure differentials, corresponding to low particle velocities. This is probably due to the fact that experimental tests #2 - 5 are all made using the rotary disk technique. Ruff and Ives¹³ state that the principal source of error using this technique would probably involve the disturbing effects of the solid disks on the flow pattern of the gas-particle mixture and would be most noticeable at low particle velocities.

The larger deviations shown in test #6 are probably due to one or more of the following reasons. (1) The particles used in this test are 160 μm silicon carbide. These particles are the smallest size tested. Khudiakov⁸ states that the smaller particles are forced toward the nozzle wall tending to slow their velocity down. (2) At low pressure differentials, the effect of the solid disks, explained above, disturb the flow pattern. (3) These small, light (low density) particles, produced the poorest (most dispersed) erosion pattern on the bottom disk. This, in turn, made the determination of the "center" of the erosion mark difficult to establish.

Variation of Particle Velocities Due to Major Particle Parameters

Some of the results of the preceding particle velocity tests are combined in Figs. VII-7 through VII-9 to illustrate the variation in particle velocities influenced by the major particle parameters of size, density and loading.

Tests #2 and 4 are combined in Fig. VII-7 to illustrate the effect of particle size on particle velocity. Both tests are made using steel shot, one with 280 μm particles and the other with 660 μm . Although the particle loading is nearly twice as great for the 660 μm test, the volume (and hence weight) of each particle is over 13 times as great. Therefore, the predominate difference between these tests is the particle size. As expected, both the program and the experimental results show the smaller particles have a greater exit velocity than the larger particles at all pressure differentials.

In a similar manner, tests #2 and 5 are combined in Fig. VII-8 to illustrate the effect of particle density on the particle velocity. The particles in both tests are 280 μm in diameter, one being steel shot (7.85 gm/cm^3) and the other silicon carbide (3.20 gm/cm^3). Again, as expected, the program and experimental results show the lower density particles have a greater exit velocity than the higher density particles.

Figure VII-9 combines tests #2 and 3 to illustrate the actual effect of particle loading on the particle velocity. Both tests are run using 280 μm steel shot. Only the particle loading, and hence the loading factor, is different.

As pointed out in Section IV, the loading factor (\dot{m}_p / \dot{m}_g) does not remain constant with a constant particle loading (\dot{m}_p) but varies as a function of differential pressure (or \dot{m}_g). Figure IV-2 illustrates how drastic the particle velocities could differ if a constant loading factor is used. Figure VII-9, however, shows that the difference in particle velocities is relatively small using constant particle loading, which produces decreasing loading factors with increasing ΔP .

Even though the velocity difference is small, the use of measured loading factors in the program, produces a good correlation between theoretical and experimental results at both loadings. This further substantiates the importance of using accurate loading factors as input to the computer program.

VIII. CONCLUSIONS AND RECOMMENDATIONS FOR FURTHER RESEARCH

Use of Verified Computer Program in Place of Experimental Measurements

A computer model of a one-dimensional two-phase particulate flow system has been successfully adapted and modified, for use with one-dimensional blast testers, to theoretically predict the exit velocity of solid particles at low temperatures and pressures. Use of this experimentally verified program eliminates the need to physically measure particle velocities, saving both time and money. An experimenter need only input the appropriate data to physically describe the equipment and conditions of a test to be run, along with the necessary loading conditions, to obtain particle velocities within the accuracy of experimental methods.

Current Use of Program

In the research program, of which this study is a part of, the mechanisms of erosion are investigated in order to establish material design criteria for the development of more economically efficient alloys and refractories. Three facets of this research project entail the need for the computer program developed in this study.

The design of a new experimental blast tester was aided by the use of this program. Given appropriate initial conditions, the optimum length of the blast tube was determined, such that the final particle velocity and final particle and gas temperatures would be within the range of conditions to be investigated.

In the study of the mechanisms of erosion conducted by McFadden¹⁴ and the effect of microstructure on solid particle erosion conducted by Brass¹⁵, the velocity of solid particles had to be controlled, such that

any chosen velocity could be obtained by making the appropriate adjustments to the equipment. This requirement was easily accomplished with the aid of this program.

For any particle and any specified hopper inclination and pressure, a loading test was run over a differential pressure span which would produce particle velocities greater than those needed. With this information and other necessary input, the program predicted the particle velocities as a function of differential pressure. Now, for the condition for which this program was run, any specified particle velocity could be obtained by simply setting the appropriate differential pressure.

Recommendations for Further Research

Although the program modified in this study has parameters for high temperature and high velocity, experimentation has not been performed to verify its accuracy. One notable parameter, the compressibility factor which expresses departures from the perfect gas law, has not been incorporated. Tests run at high pressure (> 15 psi) should definitely account for this factor. Addition of this parameter and experimentation at high temperature and pressure, should provide experimenters with a powerful tool for particle velocity prediction in one-dimensional two-phase flow.

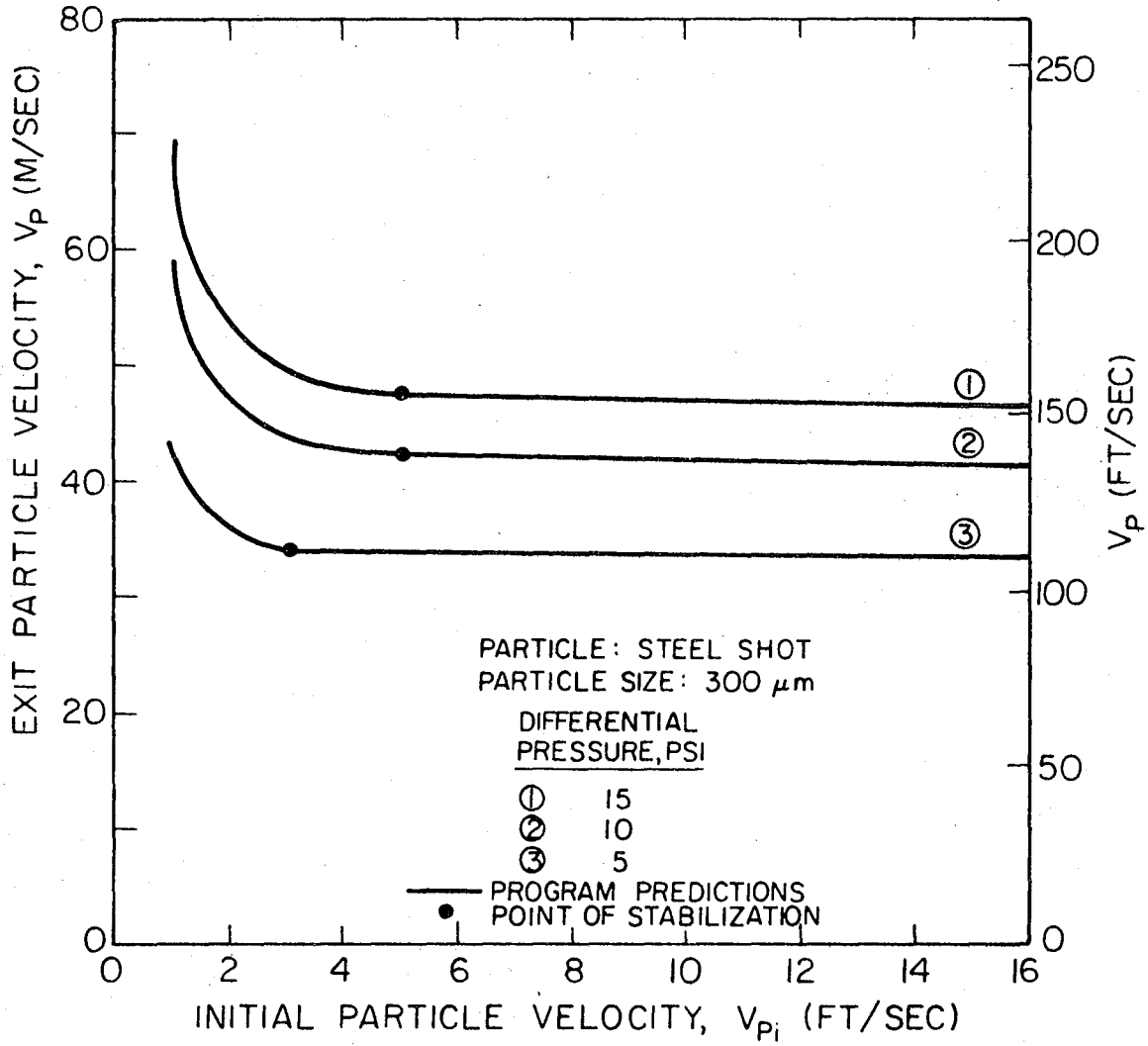
The concepts developed here for two-phase flow should be expanded to the more common cases of two or three dimensional flow for the study of particle velocities and trajectories at various locations in a flow system. For example, this analysis could be of value in predicting erosion in pipe bends.

REFERENCES

1. I. Finnie, "Erosion of Surfaces by Solid Particles", Wear 3,87-103 (1960).
2. W. Tabakoff, M. F. Hussein, "Effect of Suspended Solid Particles on the Properties in Cascade Flow", AIAA Journal 9, No. 8, 1514-1519 (1971).
3. G. P. Tilly, "Calculations of Particle Trajectories in Relation to Sand Erosion", National Gas Turbine Establishment, Note No. 729, (1968).
4. J. S. Mason, B. V. Smith, "The Erosion of Bends by Pneumatically Conveyed Suspensions of Abrasive Particles", Powder Technology 6, 323-335, (1972).
5. G. L. Sheldon, "Erosion of Brittle Materials", PhD Thesis, University of California, Berkeley, CA, (1965).
6. G. Grant, W. Tabakoff, "Erosion Prediction in Turbomachinery Due to Environmental Solid Particles", University of Cincinnati Technical Report, AIAA Paper No. 74-16, (1974).
7. IIT Research Institute, "Phase IV, Erosion-Corrosion Tests on Materials for Coal Gasification, MPC Contract No. 875-2", IITRI-B6131B05-5, (1975).
8. G. N. Khudiakov, "On the Motion of Solid Particles in Gaseous Suspension", Akademiia Nauk S.S.S.R., Otdelenie Tekhnicheskikh Nauk, No. 7, 1022-1034, (1953).
9. G. P. Tilly, "Erosion Caused by Airborne Particles", Wear 14, 63-79, (1969).

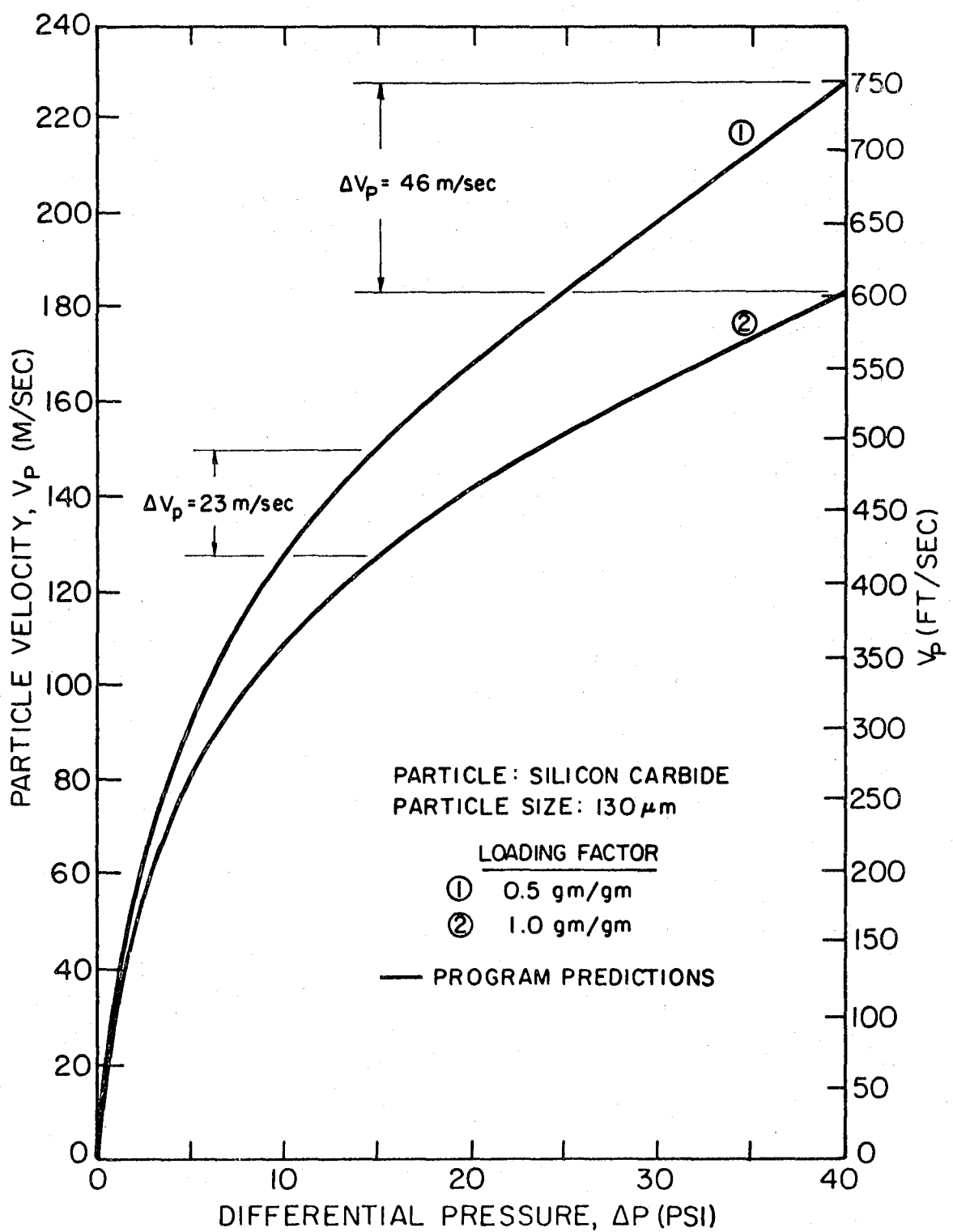
10. D. L. Martlew, "The Distribution of Impacted Particles of Various Sizes on the Blades of a Turbine Cascade", National Gas Turbine Establishment, Memorandum No. M. 274, (1956).
11. J. R. Kliegel, "Gas Particle Nozzle Flows", Ninth Symposium (International) on Combustion, Academic Press, 811-826, (1963).
12. C. T. Crowe, Personal Notes of Program for Gas-Particle Flow in a One-Dimensional Duct, M. E. Dept., Washington State University, Pullman, WA.
13. A. W. Ruff, L. K. Ives, "Measurement of Solid Particle Velocity in Erosive Wear", Wear 35, 195, (1975).
14. D. H. McFadden, "Erosion of Ductile Metals by Solid Particles", M. S. Thesis, University of California, Berkeley, CA, (1977).
15. L. Brass, "The Effects of Microstructure of Ductile Alloys on Solid Particle Erosion", M. S. Thesis, University of California, Berkeley, CA, (1977).
16. R. G. Boothroyd, Flowing Gas-Solids Suspensions, Chapman and Hall LTD, London, (1971).
17. C. T. Crowe, W. R. Babcock, P. G. Willoughby, "Drag Coefficient for Particles in Rarefied, Low Mach Number Flow", Progress in Heat and Mass Transfer, Vol. 6, 419-431, (1976).

FIGURES



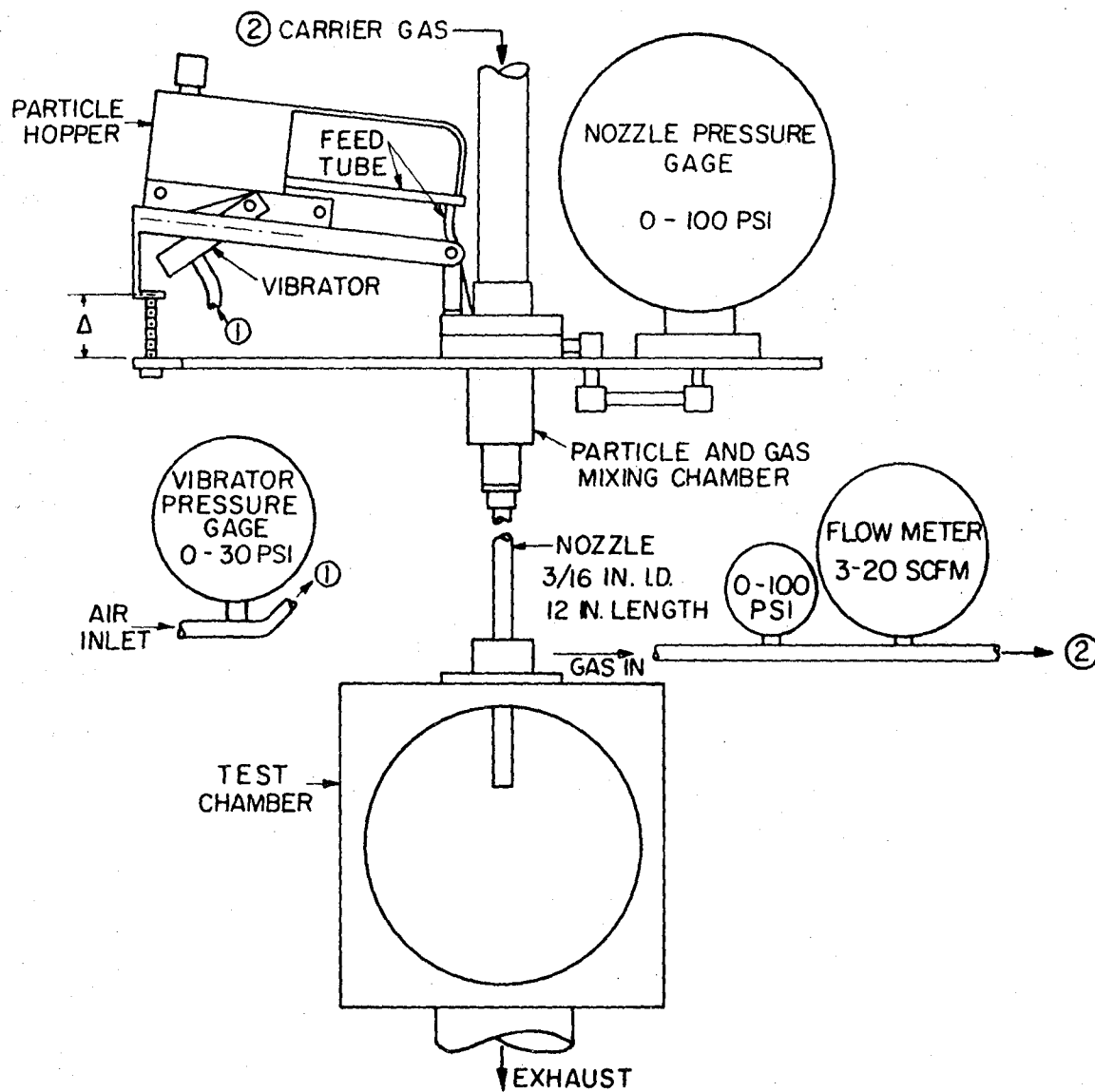
XBL 7710-6166

Figure IV-1. Effect of initial particle velocity on exit particle velocity.



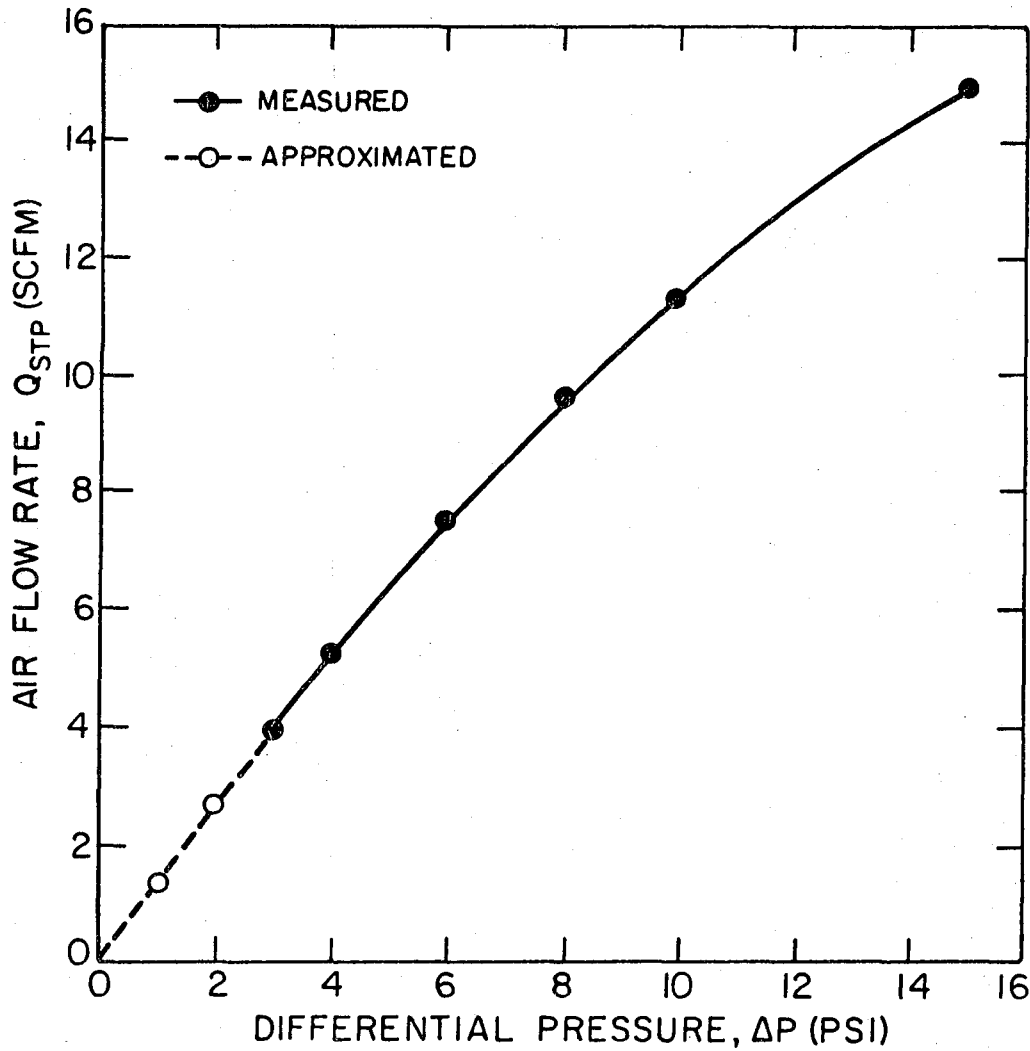
XBL 7710-6177

Figure IV-2. Predicted particle velocity variation with constant loading factor.



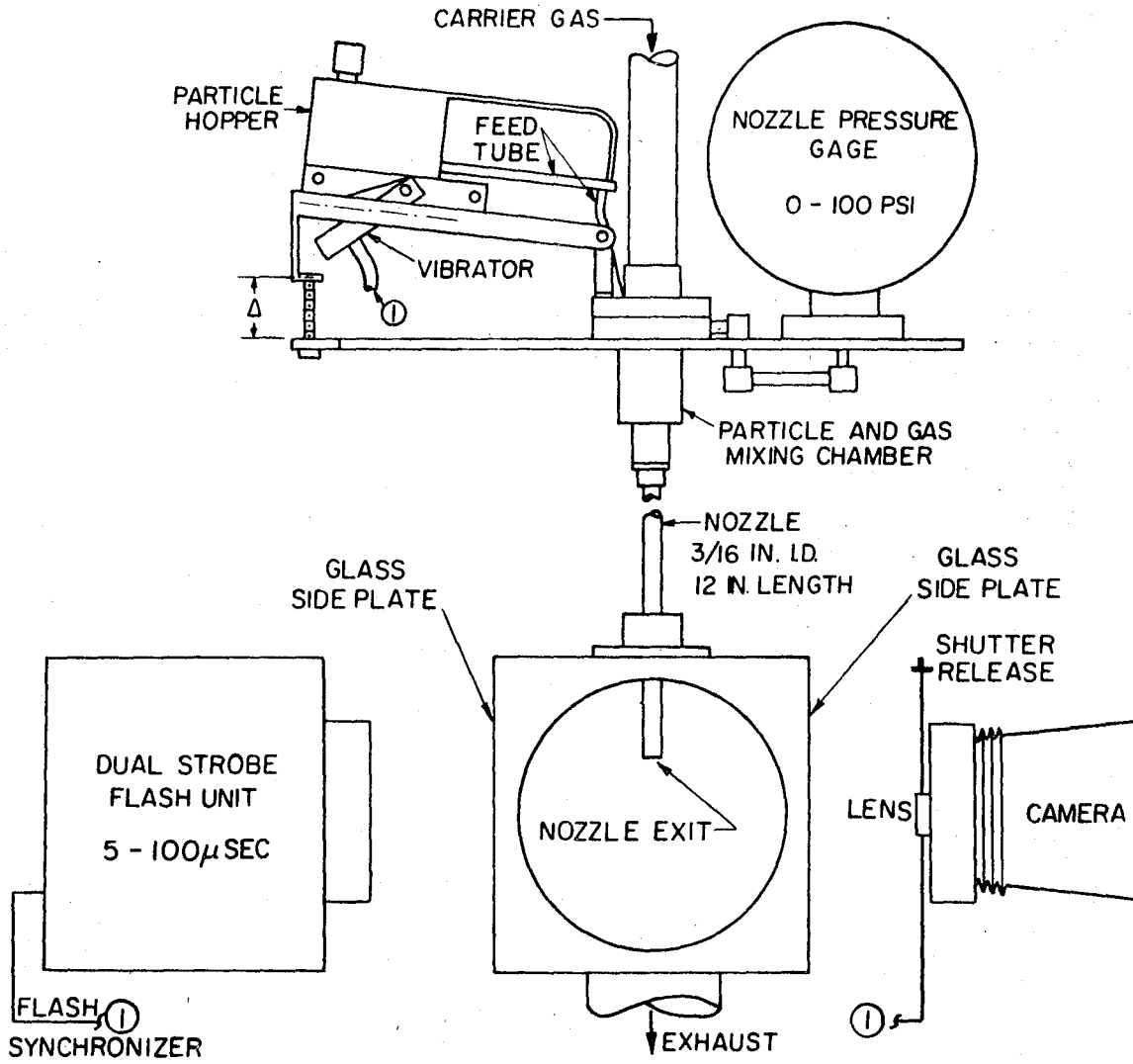
XBL 7710-6179

Figure V-1. Basic components of blast tester.



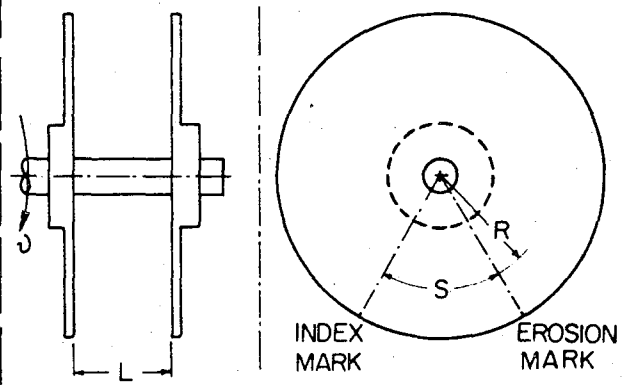
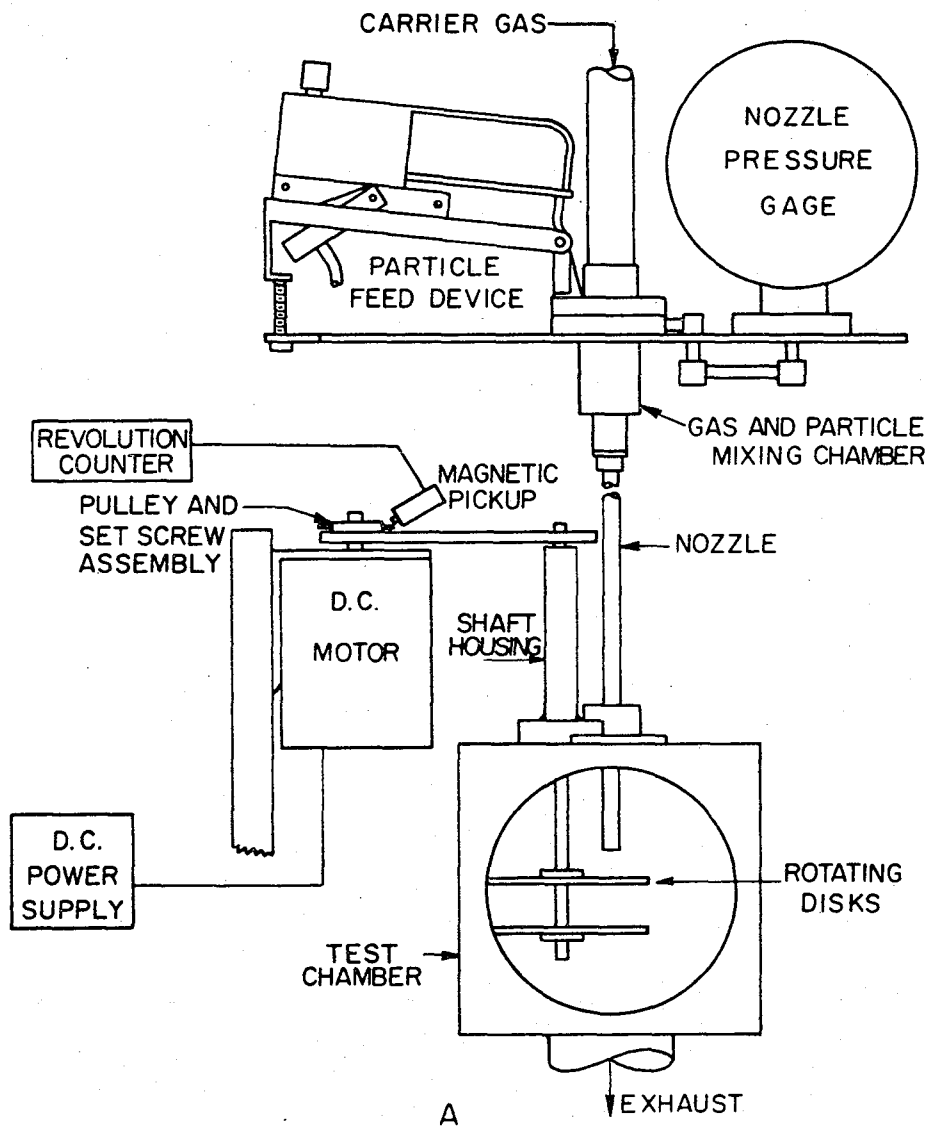
XBL 7710-6176

Figure V-2. Approximation of air flow rate at low Δp .



XBL 7710-6178

Figure V-3. Camera and flash set-up for particle velocity determination.

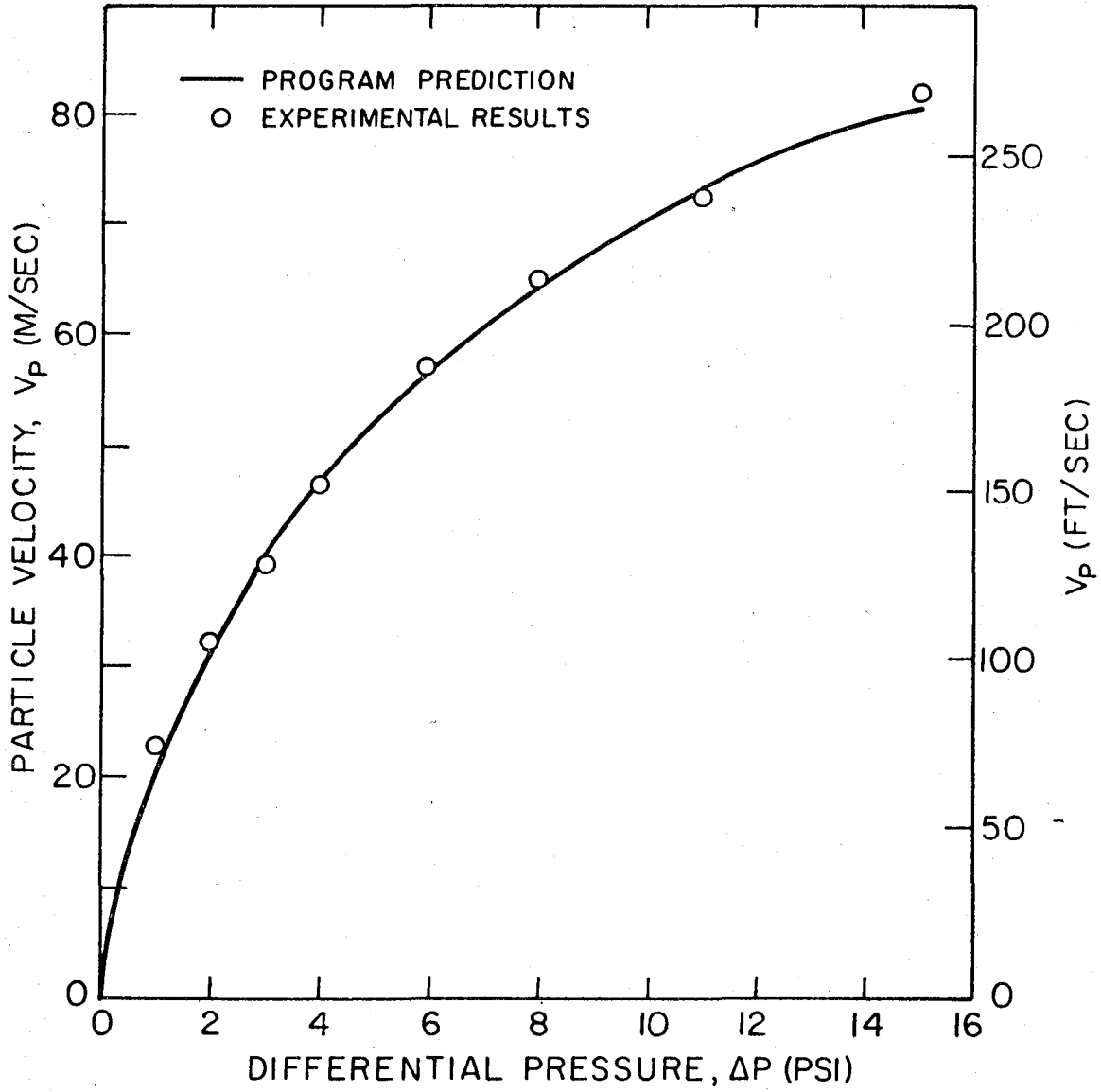


L = DISK SEPARATION
 S = ARC LENGTH BETWEEN EROSION MARKS
 R = RADIUS TO ARC LENGTH
 ν = ANGULAR VELOCITY - REV/SEC
 V_p = PARTICLE VELOCITY
 $= 2\pi R\nu L/S$

Figure V-4. A. Rotary disk set-up for particle velocity determination.
 B. Definitions of parameters used in rotary disk particle velocity calculation.

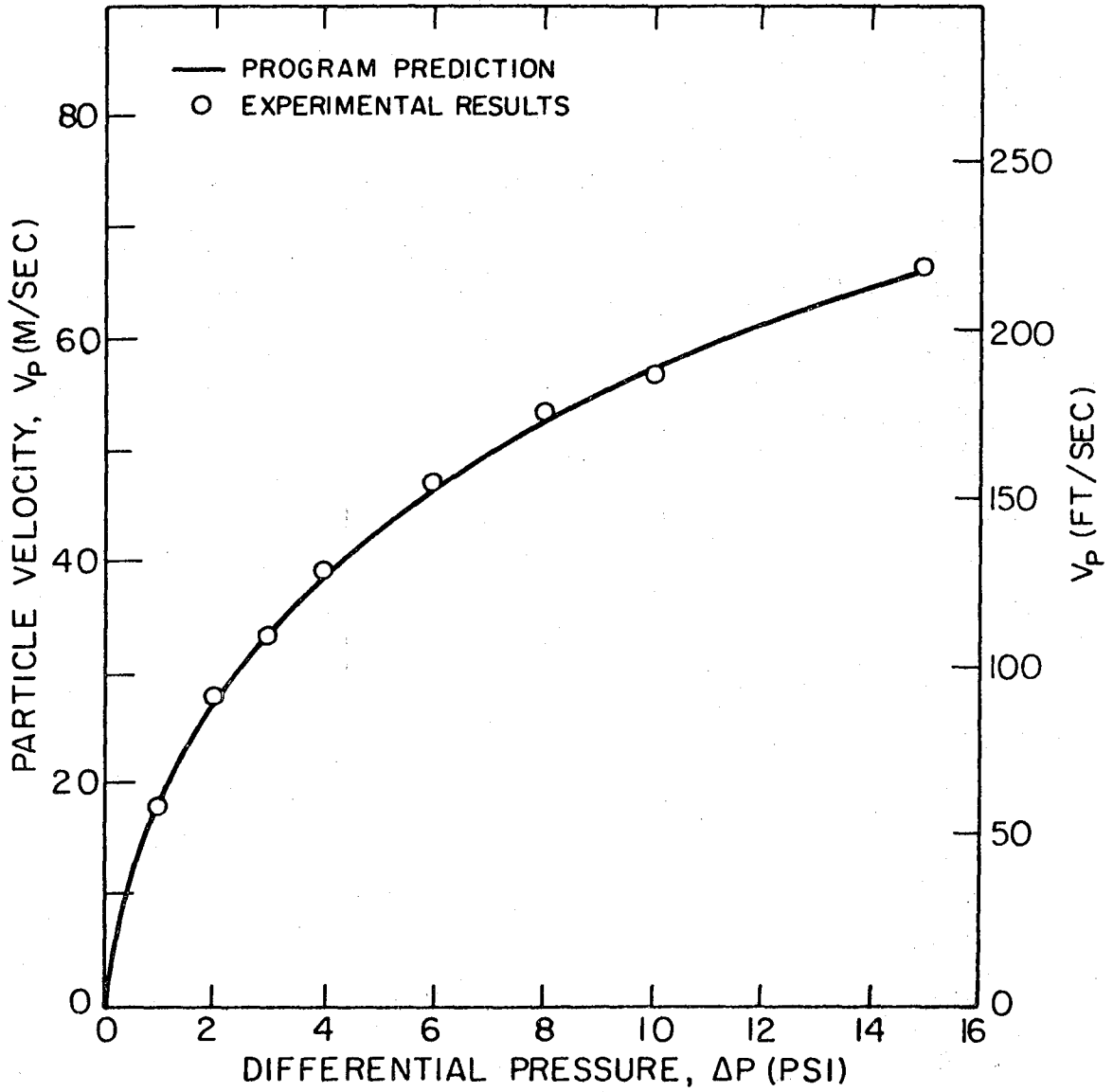
XBL 775-5524

00004903205



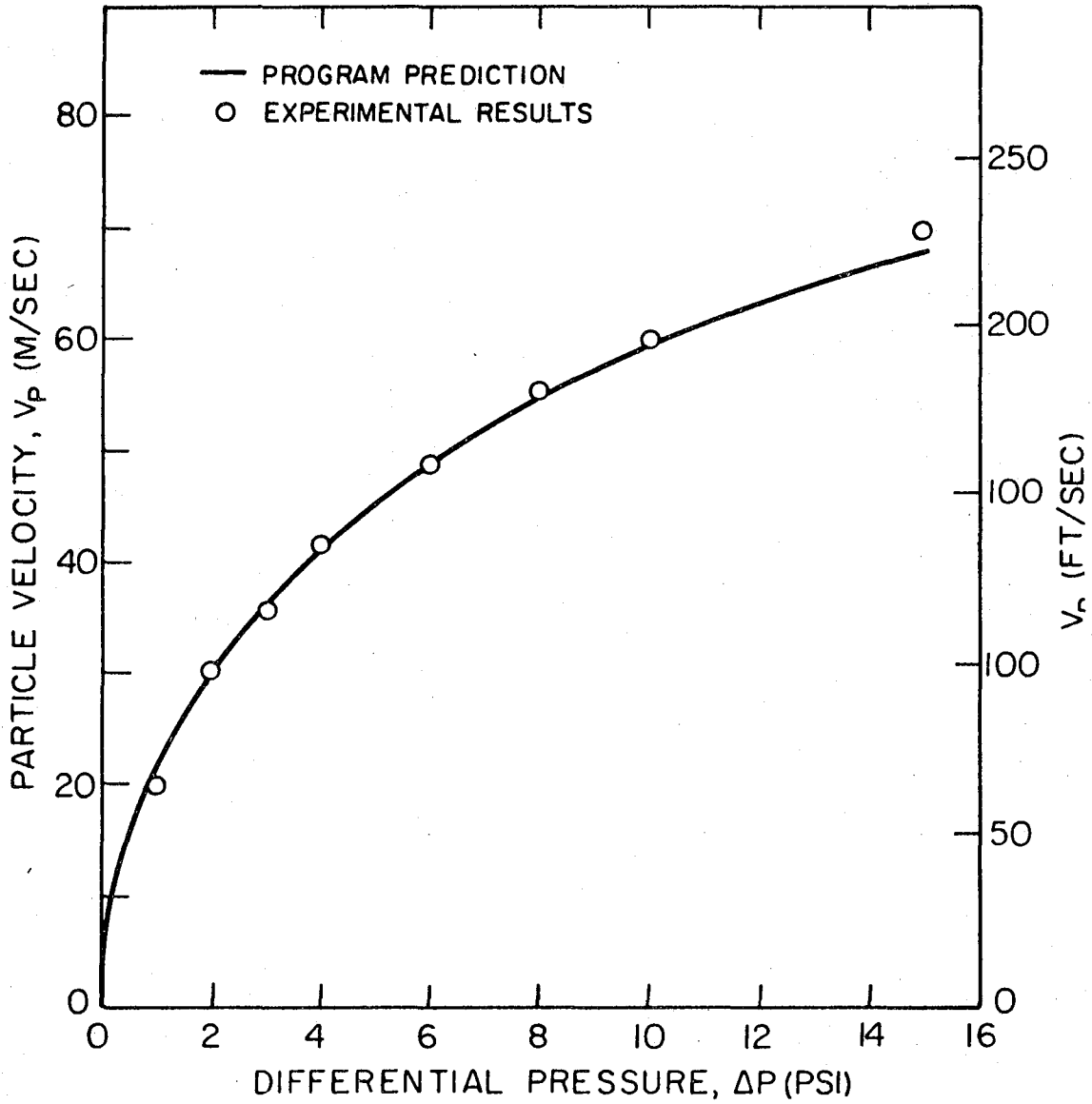
LBL7710-6175

Figure VII-1. Theoretical - experimental comparison
Test #1: 500 μm - glass sphere @ 1.15 gm/sec.



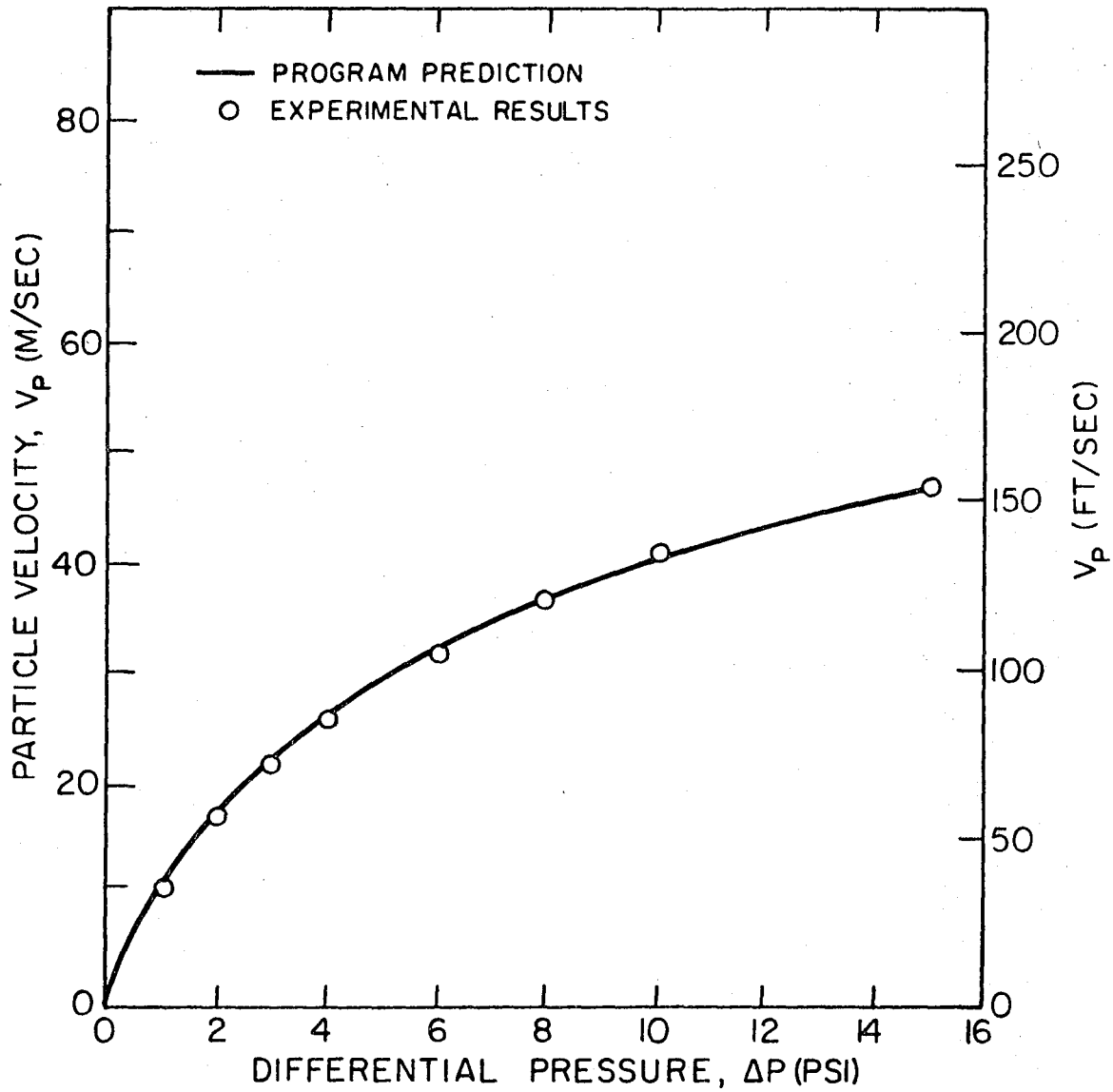
XBL7710-6174

Figure VII-2. Theoretical - experimental comparison
Test #2: 280 μm - steel shot @ 1.31 gm/sec.



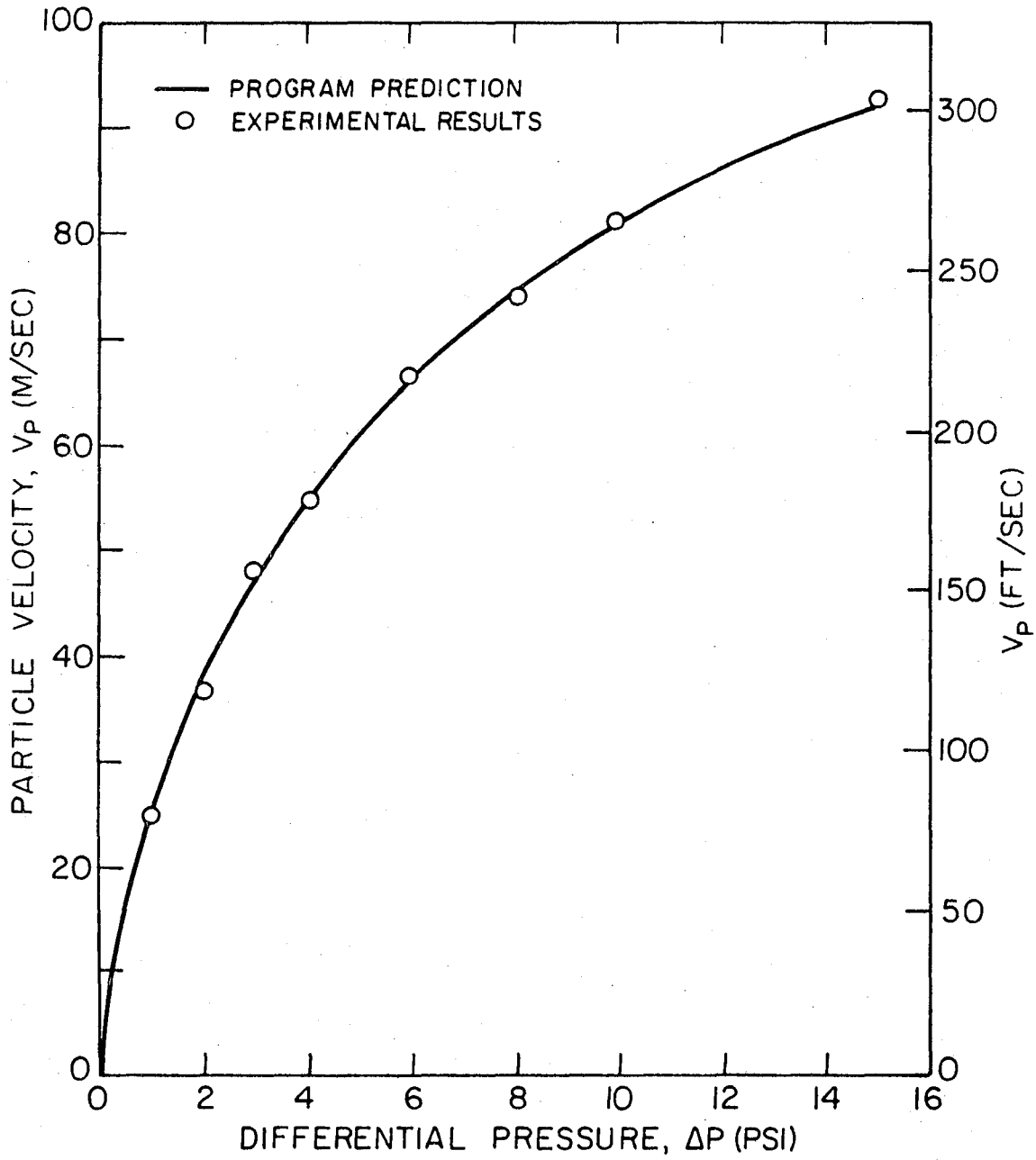
XBL 7710-6173

Figure VII-3. Theoretical - experimental comparison
Test #3: 280 μm - steel shot @ 0.11 gm/sec.



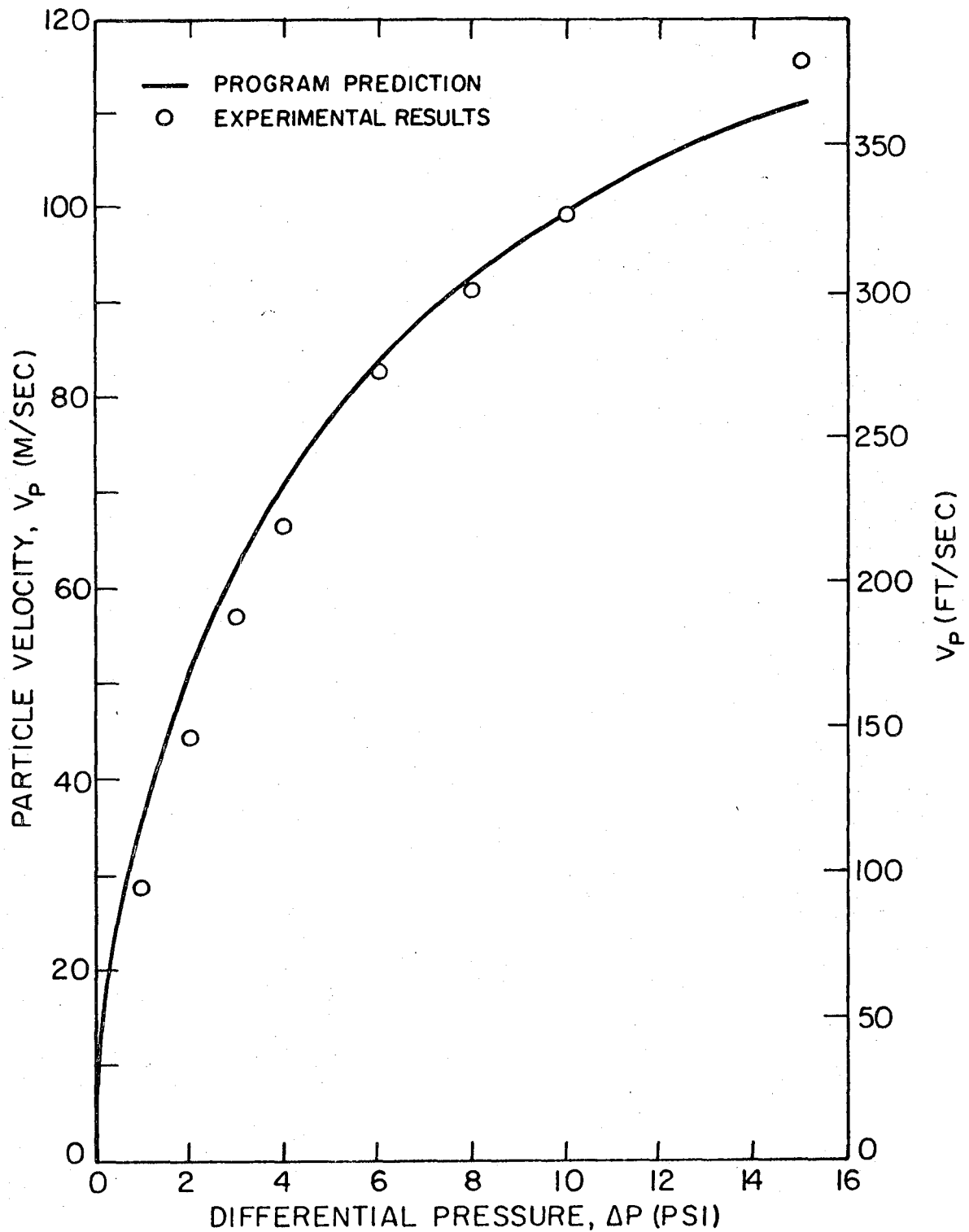
XBL 7710-6172

Figure VII-4. Theoretical - experimental comparison
Test #4: .660 μm - steel shot @ 2.32 gm/sec.



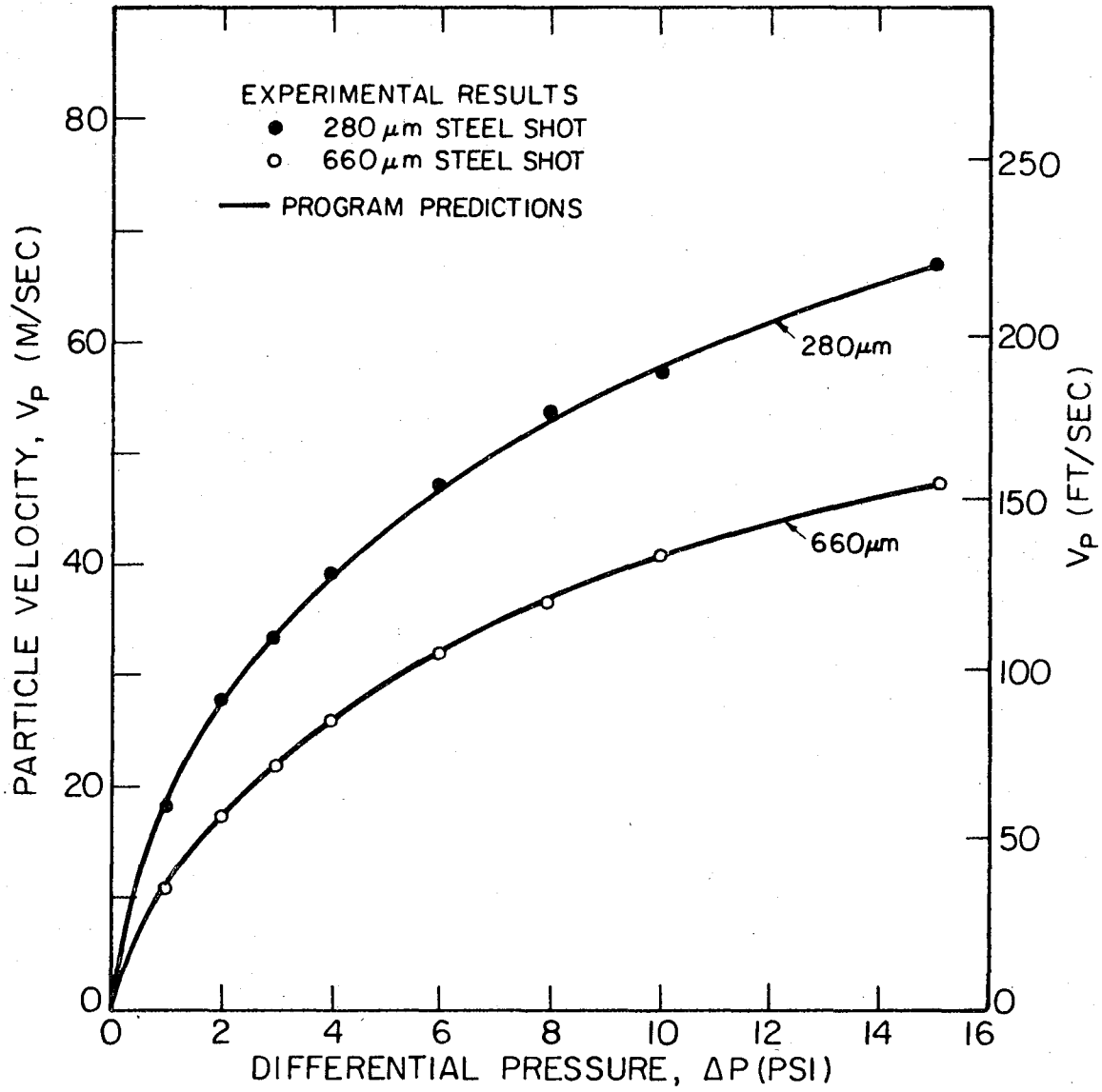
XBL7710-6171

Figure VII-5. Theoretical - experimental comparison
Test #5: 280 μm - silicon carbide @ 0.64 gm/sec.



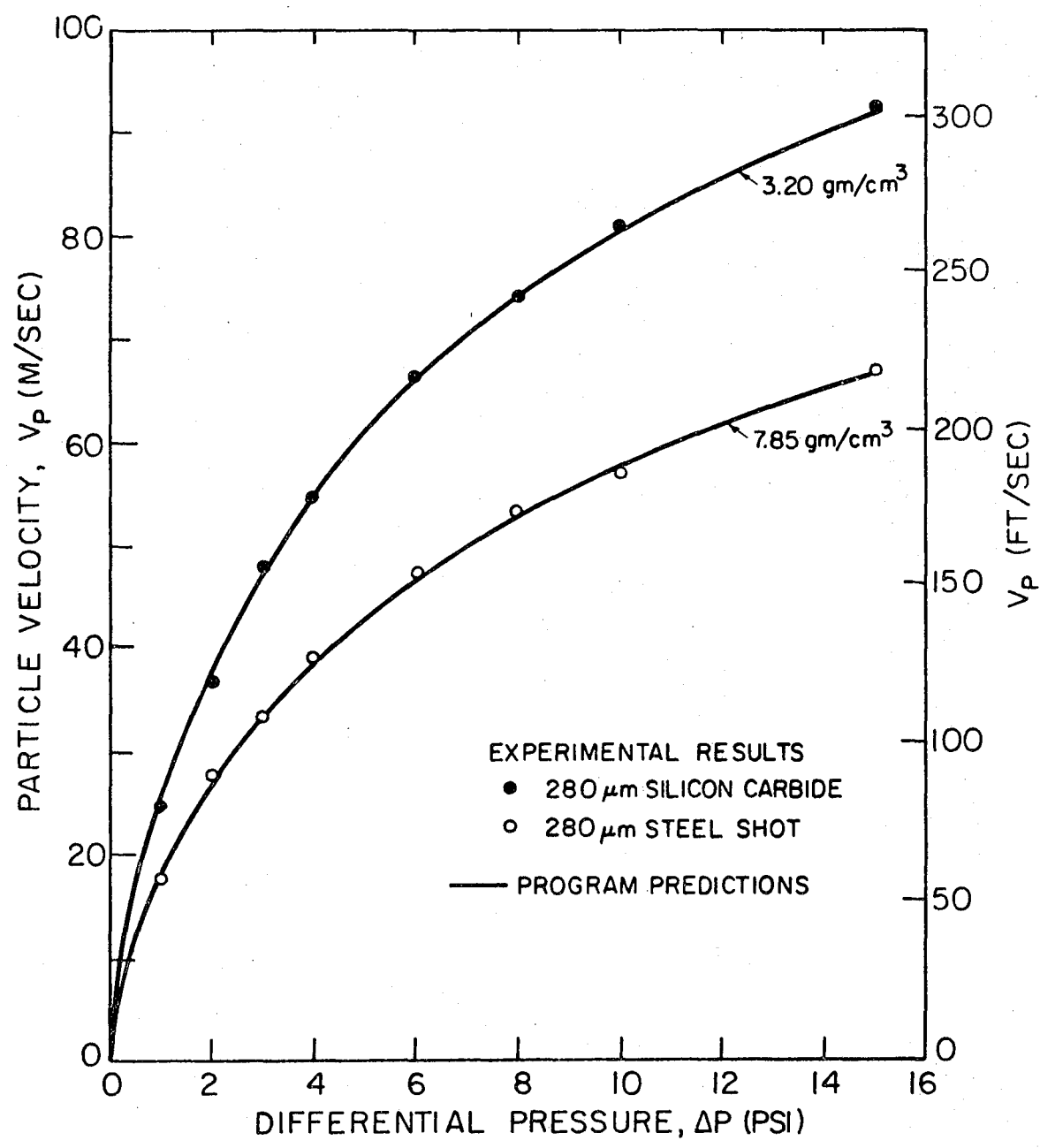
XBL 7710-6170

Figure VII-6. Theoretical - experimental comparison
Test #6: 160 μm - silicon carbide @ 0.54 gm/sec.



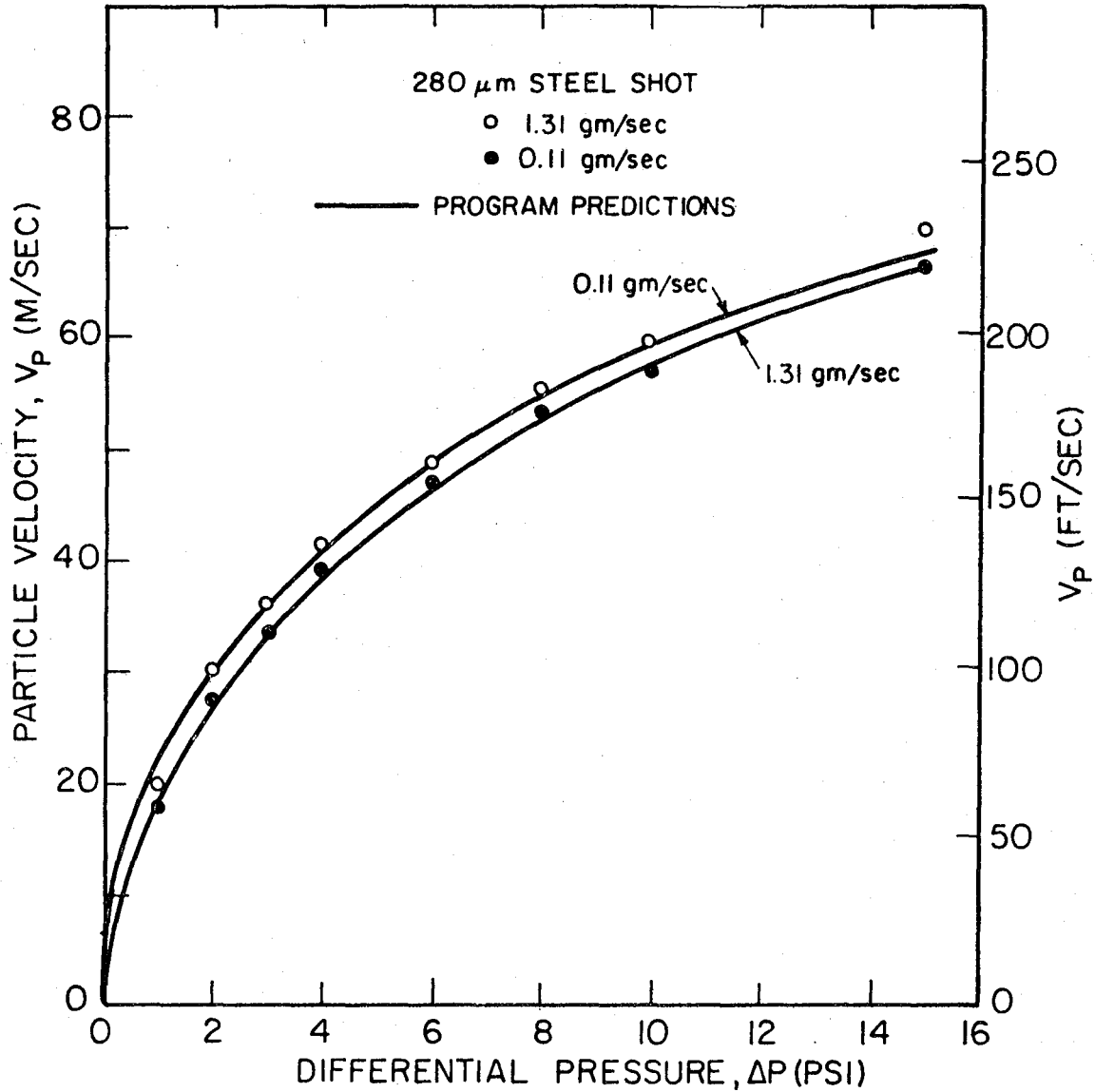
XBL7710-6169

Figure VII-7. Variation of particle velocity with particle size same particle: steel shot - different size: 280/660 μm .



XBL7710-6168

Figure VII-8. Variation of particle velocity with particle density. Same size: 280 μm - different particle: SiC/steel shot.



XBL7710-6167

Figure VII-9. Variation of particle velocity with particle loading. Same particle: steel shot - same size: 280 μm .

APPENDICES

BASIC EQUATIONS UTILIZED BY CROWE

Nomenclature

C_D	drag coefficient of particles
C_{pp}	specific heat of gas at constant pressure
C_p	specific heat of particles
D	diameter of nozzle
d_p	diameter of particles
dt	differential time
dx	differential length
F	drag force foactor: $C_D \cdot Re_p / 24$
f	D'arcy-Weisbach friction factor
h	enthalpy: $[\gamma/(\gamma-1)](p/\rho)$
k	thermal conductivity of gas
Nu	Nusselt number of gas flow in nozzle: $0.023Re^{.8}$
Nu_p	Nusselt number of gas flow around sphere: $2 + .37Re_p^{.6}$
p	pressure of gas
R	gas constant
Re	flow Reynolds number: $\rho u D / \mu$
Re_p	particle Reynolds number: $\rho_p d_p (u - u_p) / \mu$
T	temperature of gas
T_p	temperature of particles
T_w	constant wall temperature
u	gas velocity
u_p	particle velocity
γ	specific heat ratio of gas

- ρ density of gas
- ρ_p density of particles
- μ dynamic viscosity of gas.

The basic equations of fluid mechanics, thermodynamics and heat transfer that were utilized by Crowe in the derivation of the computer model are listed here for background information. The parameters with an asterisk (*) are determined by techniques presented in Section III.

Gas Only

The continuity, momentum and energy equations for inviscid, adiabatic compressible flow in a one-dimensional duct can be written as:

$$\begin{aligned}\rho u &= \text{const} \\ p + \rho u^2 &= \text{const} \\ \rho u(h + u^2/2) &= \text{const.}\end{aligned}$$

The fourth equation necessary to complete the set is the equation of state:

$$p = \rho RT.$$

Also, assuming the gas is calorically perfect:

$$h = C_p T.$$

The effect of wall friction reduces the momentum of the gas:

$$\frac{d}{dx} (p + \rho u^2) = -\frac{1}{2} f^* \rho u^2 / D.$$

The heat transfer between the gas and the wall of the duct, effects the energy of the gas:

$$\frac{d}{dx} [\rho u(h + u^2/2)] = \frac{4Nu^* k^* (T_w - T)}{D^2} .$$

Extension to Gas-Particle Flow

The gas will accelerate a particle by aerodynamic drag forces at the expense of losing momentum in the same direction. The coupling equation necessary is the particle-trajectory equation:

$$u \frac{du_p}{dx} = \frac{C_D^* Re_p}{24} \cdot \frac{18\mu^*}{\rho_p d_p^2} (u - u_p).$$

The heat transfer between the particles and the gas effect the energy of the system. The coupling equation necessary is the particle time-temperature equation:

$$C_{pp} \frac{dT_p}{dt} = Nu_p \frac{6k^*}{\rho_p d_p^2} (T - T_p).$$

NOMENCLATURE FOR BASIC PROGRAM

- AK = Specific heat ratio, γ : 1.4 for air
- ANU = Nusselt number based on particle Reynolds number, Nu_p
- CF = Skin friction coefficient, C_f : D'arcy-Weisbach friction factor (f)/4
- CP = Specific heat of particle, C_p ($m^2/sec^2-^\circ K$)
- DEN = Initial gas density, ρ_g (kg/m^3)
- DIA = Diameter of nozzle, D (m)
- DF = Drag force factor, F: $C_D \cdot Re_p / 24$
- DGF = Statement function to update gas density (kg/m^3)
- DG(I) = Gas density, ρ_g , in cell i (kg/m^3) For I = 1; initial gas density
- DL = Length of nozzle, L (m)
- DT = Time of flight of particles through each cell, dt (sec)
- DX = Differential length of cell, dx (m)
- FFAC = Factor in momentum "sink" term
- HTC = Factor for particle heat transfer ($m^2/sec^3-^\circ K$)
- I = Cell number indicator
- NI = Nothing
- NUM = Number of cells
- PGF = Statement function to update gas pressure (N/m^2)
- PG(I) = Gas pressure, p_g , in cell i (N/m^2) For I = 1; initial gas pressure
- PNU = Nusselt number based on flow Reynolds number, Nu_f
- PRE = Initial gas pressure, p_g (N/m^2)
- QFAC = Factor for heat transfer between gas and nozzle wall ($kg/sec^3-^\circ K$)
- RE = Particle Reynolds number, Re_p

REC	= Factor used in particle Reynolds number ($m^2\text{-sec/kg}$)
RGAS	= Gas constant, R: 287 (N-m/kg-°K) for air
TC	= Thermal conductivity of gas, k (W/m-°K)
TC	= (TC used twice) Factor, quotient of τ/F (sec)
TCC	= Stokes constant, τ (sec)
TD	= Temperature difference between gas and particles (°K)
TGAS	= Initial gas temperature, T_g (°K)
TGF	= Statement function to update gas temperature (°K)
TG(I)	= Gas temperature, T_g , in cell i (°K) For I = 1; initial gas temperature
TP(I)	= Particle temperature, T_p , in cell i (°K) For I = 1; initial particle temperature
TW	= Constant wall temperature, T_w (°K)
VD	= Velocity difference between the gas and particles (m/sec)
VEL	= Initial gas velocity, V_g (m/sec)
VG(I)	= Gas velocity, V_g , in cell i (m/sec) For I = 1; initial gas velocity
VGf	= Statement function to update gas velocity (m/sec)
VP(I)	= Particle velocity, V_p , in cell i (m/sec) For I = 1; initial particle velocity
X	= Equation of mass for the gas ($kg/m^2\text{-sec}$)
Y	= Initial momentum equation for gas ($kg/m\text{-sec}^2$)
YG(I)	= Momentum equation for gas at cell i ($kg/m\text{-sec}^2$) For I = 1; initial momentum equation for gas
Z	= Initial energy equation for gas (kg/sec^3)
ZG(I)	= Energy equation for gas at cell i (kg/sec^3) For I = 1; initial energy equation for gas

CROWE'S BASIC PROGRAM: GAS ONLY

```
//          JOB(,3), 'CROWE', CLASS=A
// EXEC WATFIV
//GO.SYSIN DD *
$JOB
C THIS IS A CLASS PROBLEM FOR ME 549-TWO PHASE FLOW
  DIMENSION VG(50), VGO(50), DG(50), PG(50), YG(50), ZG(50), TG(50),
  LCHYG(50)
  VGF(AK, Y, X, Z)=(AK*Y)/((AK+1.)*X)*(1.-SQRT(1.-2*(AK**2-1.)
  1*X*Z/(AK*Y)**2))
  DGF(X, VEL)=Y/VEL
  PGF(X, VEL, Y)=Y-X*VEL
  TGF(DEN, RGAS, PRE)=PRE/(DEN*RGAS)
  RGAS=287.
  AK=1.4
  X=33.75
  Y=500506.25
  Z=26253796.43
  VEL=VGF(AK, Y, X, Z)
  DEN=DGF(X, VEL)
  PRE=PGF(X, VEL, Y)
  TGAS=TGF(DEN, RGAS, PRE)
  CF=.002
  TC=.0566
  PHU=507.
  TW=573.
  DL=6.
  DIA=.3
  NUM=50
  NI=0
  DX=DL/FLOAT(NUM-1)
  FFAC=2*CF*DX/DIA
  QFAC=TC*PNU*4*DX/DIA**2
  VG(1)=VEL
  DG(1)=DEN
  PG(1)=PRE
  YC(1)=Y
  ZG(1)=Z
  TG(1)=TGAS
  DO 50 I=2, NUM
  YG(I)=YG(I-1)-FFAC*DG(I-1)*YG(I-1)**2
  ZG(I)=ZG(I-1)-QFAC*(TG(I-1)-TW)
  VG(I)=VGF(AK, YG(I), X, ZG(I))
  DG(I)=DGF(X, VG(I))
  PG(I)=PGF(X, VG(I), YG(I))
50 TG(I)=TGF(DG(I), RGAS, PG(I))
  WRITE(6,1) (VG(I), DG(I), PG(I), TG(I), I=1, NUM)
  1 FORMAT('          VELOCITY          DENSITY          PRESSURE
  1          TEMPERATURE'//(4(2X, F13.2)))
  STOP
  END
```

\$DATA

//

CROWE'S BASIC PROGRAM: GAS-PARTICLE FLOW

```

//          JOB (,3), 'CROWE', CLASS=A
// EXEC WATFIV
//GO.SYSIN DD *
$JOB
C THIS IS A CLASS PROBLEM FOR ME549-TWO PHASE FLOW
  DIMENSION VG(50), TP(50), DG(50), PG(50), YG(50), ZG(50), TG(50),
  1VP(50)
  VGF(AK, Y, X, Z)=(AK*Y)/((AK+1.)*X)*(1.-SQRT(1.-2*(AK**2-1.)
  1*X*Z/(AK*Y)**2))
  DGF(X, VEL)=X/VEL
  PGF(X, VEL, Y)=Y-X*VEL
  TGF(DEN, RGAS, PRE)=PRE/(DEN*RGAS)
  RGAS=287.
  AK=1.4
  X=33.75
  Y=500506.25
  Z=26253796.43
  REC=6.097
  TCC=.532
  HTC=1080.
  CP=1025.
  VEL=VGF(AK, Y, X, Z)
  DEN=DGF(X, VEL)
  PRE=PGF(X, VEL, Y)
  TGAS=TGF(DEN, RGAS, PRE)
  CF=.002
  TC=.0566
  PNU=507.
  TW=573.
  DL=6.
  DIA=.3
  NUM=50
  NI=0
  DX=DL/FLOAT(NUM-1)
  FFAC=2*CF*DX/DIA
  QFAC=TC*PNU*4*DX/DIA**2
  VG(1)=VEL
  DG(1)=DEN
  PG(1)=PRE
  YG(1)=Y
  ZG(1)=Z
  TG(1)=TGAS
  VP(1)=5.
  TP(1)=973.
  DO 50 I=2, NUM
  DT=DX/VP(I-1)
  TD=TG(I-1)-TP(I-1)
  VD=VG(I-1)-VP(I-1)
  RE=REC*DG(I-1)*ABS(VD)
  DF=1.+.15*RE**.687
  TC=TCC/DF
  ANU=2.+.37*RE**.6
  YG(I)=YG(I-1)-FFAC*DG(I-1)*VG(I-1)**2-2*X*DT*VD/TC
  ZG(I)=ZG(I-1)-QFAC*(TG(I-1)-TW)-2*X*DT*ANU*HTC*TD
  VP(I)=VP(I-1)+DT*VD/TC
  TP(I)=TP(I-1)+ANU*HTC*DT*TD/CP
  VG(I)=VGF(AK, YG(I), X, ZG(I))

```

```
DG(I)=DGF(X, VG(I))
PG(I)=PGF(X, VG(I), YG(I))
50 TG(I)=TGF(DG(I), RGAS, PG(I))
WRITE(6,1) (VG(I), DG(I), PG(I), TG(I), TP(I), VP(I), I=1, NUM)
1 FORMAT('          VELOCITY          DENSITY          PRESSURE
1          TEMPERATURE    PART TEMP    PART VEL'//(6(2X, F13.2)))
STOP
END
```

\$DATA

//

NOMENCLATURE FOR MODIFIED PROGRAM

AK	= Specific heat ratio, γ : 1.4 for air
ANU	= Nusselt number based on particle Reynolds number, Nu_p
AREA	= Cross-sectional area of nozzle, A (ft^2) (m^2)
ARG	= Argument of SQRT term in statement function VGF
AT	= Coefficient a_1 in thermal conductivity expression
AU	= Coefficient a_1 in gas viscosity expression
BT	= Coefficient a_2 in thermal conductivity expression
BU	= Coefficient a_2 in gas viscosity expression
C	= Factor for Mach number effects between particles and gas
CCP	= Specific heat of particle, C_p ($Btu/lb_m-\circ R$) ($J/kg-\circ K$)
CF	= Skin friction coefficient, C_f : D'arcy-Weisbach friction factor (f)/4
CP	= Specific heat of particle, C_p ($ft^2/sec^2-\circ R$) ($m^2/sec^2-\circ K$)
CT	= Coefficient a_3 in thermal conductivity expression
CU	= Coefficient a_3 in gas viscosity expression
DDL	= Incremental length of nozzle, dL (in) (cm)
DEN	= Initial gas density, ρ_g (lb_m/ft^3) (kg/m^3)
DENP	= Actual density of particles, ρ_p (lb_m/ft^3) (kg/m^3)
DIA	= Diameter of nozzle, D (ft) (m)
DIACM	= Diameter of nozzle, D (cm)
DIAI	= Diameter of nozzle, D (in)
DIF	= Differential pressure, ΔP (psi) (N/m^2)
DIFP	= Differential pressure, ΔP (lb_f/ft^2) (N/m^2)
DF	= Drag force factor, F : $C_D \cdot Re_p / 24$
DGF	= Statement function to update gas density (lb_m/ft^3) (kg/m^3)

DG(I)	= Gas density, ρ_g , in cell i (lb_m/ft^3) (kg/m^3) For I = 1; Initial gas density
DL	= Length of nozzle, L (ft) (m)
DP	= Diameter of particle, d_p (ft) (m)
DPM	= Diameter of particle, d_p (μm)
DPRE	= Differential pressure increment, ΔP (psi) (N/m^2)
DT	= Time of flight of particles through each cell, dt (sec)
DX	= Differential length of cell, dx (ft) (m)
FFAC	= Factor in momentum "sink" term
FL	= Loading factor, \dot{m}_p/\dot{m}_g (lb_p/lb_g) (gm_p/gm_g)
HTC	= Factor for particle heat transfer ($\text{ft}^2/\text{sec}^3\text{-}^\circ\text{R}$) ($\text{m}^2/\text{sec}^3\text{-}^\circ\text{K}$)
I	= Cell number indicator- Main program
J	= Cell number indicator- Output
K	= Differential pressure increment multiplier
L	= Nozzle length increment multiplier
M	= Data card input counter
NI	= Indicator set if particle velocity exceeds gas velocity
NUM	= Number of cells
PGF	= Statement function to update gas pressure (lb_f/ft^2) (N/m^2)
PG(I)	= Gas pressure, p_g , in cell i (lb_f/ft^2) (N/m^2) For I = 1; initial gas pressure
PNU	= Nusselt number based on flow Reynolds number, Nu_f
PRE	= Initial gas pressure, p_g (lb_f/ft^2) (N/m^2)
PRED	= Acceptable tolerance for difference between calculated and actual exit gas pressure (lb_f/ft^2) (N/m^2)
PREF	= Actual exit gas pressure (lb_f/ft^2) (N/m^2)
QFAC	= Factor for heat transfer between gas and nozzle wall ($\text{lb}_m/\text{sec}^3\text{-}^\circ\text{R}$) ($\text{kg}/\text{sec}^3\text{-}^\circ\text{K}$)

QSTP	= Flow rate of gas at standard temperature and pressure (ft ³ /sec) (m ³ /sec)
RE	= Flow Reynolds number, Re
REC	= Factor used in particle Reynolds number (ft ² sec/lb _m) (m ² sec/kg)
REP	= Particle Reynolds number, Re _p
RGAS	= Gas Constant, R: 53.35 (ft-lb _f /lb _m -°K) or 287 (Nm/kg-°K) for air
TC	= Thermal conductivity of gas, k (ft-lb _f /ft-sec-°R) (W/m-°K)
TCC	= Stokes constant, τ (sec)
TCL	= Factor, quotient of τ/F (sec)
TD	= Temperature difference between gas and particles (°R) (°K)
TGAS	= Initial gas temperature, T _g (°R) (°K)
TGASC	= Initial gas temperature, T _g (°C)
TGASF	= Initial gas temperature, T _g (°F)
TGF	= Statement function to update gas temperature (°R) (°K)
TG(I)	= Gas temperature, T _g , in cell i (°R) (°K) For I = 1; initial gas temperature
TP(I)	= Particle temperature, T _p , in cell i (°R) (°K) For I = 1; initial particle temperature
TR	= Conversion from(°K) to (°R) of gas temperature for use in interpolating polynomials in S.I. program (°R)
TW	= Constant wall temperature, T _w (°R) (°K)
TWC	= Constant wall temperature, T _w (°C)
TWF	= Constant wall temperature, T _w (°F)
VC	= Check for local speed of sound in gas: 0.99a (ft/sec) (m/sec)
VD	= Velocity difference between the gas and particles (ft/sec) (m/sec)
VEL	= Initial gas velocity, V _g (ft/sec) (m/sec)

- VELL = Lower limit of velocity guess (ft/sec) (m/sec)
- VELU = Upper limit of velocity guess (ft/sec) (m/sec)
- VG(I) = Gas velocity, V_g , in cell i (ft/sec) (m/sec) For I = 1; initial gas velocity
- VGF = Statement function to update gas velocity (ft/sec) (m/sec)
- VISK = Viscosity of Gas, μ (lb_m/sec-ft) (kg/sec-m)
- VP(I) = Particle velocity, V_p , in cell i (ft/sec) (m/sec) For I = 1; initial particle velocity
- X = Equation of mass for the gas (lb_m/ft²-sec) (kg/m²-sec)
- XM = Local Mach number, M, based on velocity difference between gas and particles
- Y = Initial momentum equation for gas (lb_m/ft-sec²) (kg/m-sec²)
- YG(I) = Momentum equation for gas at cell i (lb_m/ft-sec²) (kg/m-sec²) For I = 1; initial momentum equation for gas
- Z = Initial energy equation for gas (lb_m/sec³) (kg/sec³)
- ZG(I) = Energy equation for gas at cell i (lb_m/sec³) (kg/sec³) For I = 1; initial energy equation for gas

Numerical Constants

- 777.649 = The mechanical equivalent of heat, J (lb_f-ft/Btu)
- 32.174 = Constant of proportionality in Newton's 2nd Law (lb_m-ft/lb_f-sec²)
- 3.14159 = Pi, π

CROWES

PROGRAM CROWES(INPUT,OUTPUT)

```

C SILICON CARBIDE PARTICLES-280 MICRONS,+60-48,W/LOADING VARIATIONS
  DIMENSION VG(400),DG(400),PG(400),YG(400),ZG(400),TG(400),
  IVP(400),IP(400)
C STATEMENT FUNCTIONS
  VGF(AK,Y,X,Z,ARG)=(AK*Y)/((AK+1.)*X)*(1.-SQRT(ARG))
  DGF(X,VEL)=X/VEL
  PGF(X,VEL,Y)=(Y-X*VEL)/32.174
  TGF(DEN,RGAS,PRE)=PRE/(DEN*RGAS)
  PRINT 1
C COEFFICIENTS FOR INTERPOLATING POLYNOMIAL TO DETERMINE VISK=VISK(R)
  FOR AIR.
52 AU=3.613800798E-02
53 BU=1.75335507E-04
55 CU=-2.175980811E-08
C COEFFICIENTS FOR INTERPOLATING POLYNOMIAL TO DETERMINE TC=TC(R)
  FOR AIR.
56 AT=1.257804164E-03
60 BT=2.784865154E-05
61 CT=-3.813387944E-09
C NUMBER OF STATIONS PER LENGTH OF TUBE
63 NUM=400
C GAS CONSTANTS
64 AK=1.4
65 RGAS=53.35
C INPUT DO LOOP
67 DO 15 M=1,8
71 READ 20,DPRE,DDL,TGASF,TWF,DPM,DIAI,FL
112 READ 25,DENP,CCP
122 CP=CCP*777.649*32.174
124 TGAS=TGASF+460.
126 VP(1)=5.
130 PRINT 30,DPM,VP(1),DIAI,FL
144 DIA=DIAI/12.
146 AREA=3.14159*DIA**2/4.
C DIFFERENTIAL PRESSURE DO LOOP
151 DO 14 K=1,1
152 DIFP=DPRE*K*144.
154 DIF=DIFP/144.
156 PRINT 40,DIF
C TUBE LENGTH DO LOOP
163 DO 13 L=1,1
165 DL=DDL*L/12.
C FIND GAS VELOCITY TO PRODUCE DESIRED PRESSURE DROP
167 PRED=DIFP/100.
171 PREF=2116.224
173 PRE=PREF+DIFP
174 VELL=0.
175 DEN=PRE/(RGAS*TGAS)
200 VELU=SQRT(1.4*32.174*RGAS*TGAS)
205 2 VEL=(VELL+VELU)/2.
207 VISK=(AU+RU*TGAS+CU*TGAS**2)*.0001
215 RE=VEL*DIA*DEN/VISK
217 CF=3.051187564E-01*RE**-.2.463091378E-01/4.
224 PNU=.023*RE**.8
230 X=DEN*VEL

```

CROWEE

-82-

```

232      Y=PRE*32.174*X*VEL
235      Z=X*(VEL**2/2.+AK*PRE*32.174/((AK-1.)*DEN))
      C   CHECK FOR NEGATIVE ARGUMENT OF SQUARE ROOT
245      ARG=1.-2.*(AK**2-1.)*X*Z/(AK*Y)**2
253      IF(ARG.GT.0.) GO TO 3
256      IF(ARG.LE.0.) VELU=VEL
261      GO TO 2
262      3  VEL=VGF(AK,Y,X,Z,ARG)
272      DEN=DGF(X,VEL)
274      PRE=PGF(X,VEL,Y)
277      TGAS=TGF(DEN,RGAS,PRE)
303      TC=(AT+BT*TGAS+CT*TGAS**2)*777.649/3600.
310      TW=TWf+460.
      C   ADD PARAMETERS FOR GAS-PARTICLE FLOW
312      DP=DPM*.00003937/12.
314      REC=DP/VISK
316      TCC=DENP*DP**2/(18.*VISK)
321      HTC=6.*TC*32.174/(DENP*DP**2)
324      NI=0
325      DX=DL/FLOAT(NUM-1)
330      FFAC=2*CF*DX/DIA
334      QFAC=32.174*TC*PNU*4*DX/DIA**2
341      TP(1)=535.
343      VG(1)=VEL
344      DG(1)=DEN
346      PG(1)=PRE
347      YG(1)=Y
351      ZG(1)=Z
352      TG(1)=TGAS
      C   INCREMENTING DO LOOP
354      DO 10 I=2,NUM
356      DT=DX/VP(I-1)
360      TD=TG(I-1)-TP(I-1)
362      IF(NI.EQ.1) GO TO 6
364      VD=VG(I-1)-VP(I-1)
366      IF(NI.EQ.0) GO TO 4
367      GO TO 6
      C   MACH NUMBER EFFECTS
367      4  XM=ABS(VD/(SQRT(1.4*32.174*53.35*1G(I-1))))
375      C=1.65+.65*TANH(2.*ALOG(XM))+.425*EXP(-2.5*(ALOG(XM/1.4))**2)
416      REP=REC*DG(I-1)*ABS(VD)
422      IF(REP.LE.200.) GO TO 5
425      IF(REP.LE.2500.) DF=(21.9416*REP**+.718+.324)*REP*C/24.
440      IF(REP.GT.2500.) DF=.4*REP*C/24.
446      GO TO 7
447      5  DF=(1.+15*REP**+.687)*C
456      GO TO 7
456      6  VD=0.
457      DF=1.
462      7  TC1=TCC/DF
464      ANU=2.+37*REP**+.6
472      YG(I)=YG(I-1)-FFAC*DG(I-1)*VG(I-1)**2-FL*X*DT*VD/TC1
502      ZG(I)=ZG(I-1)-QFAC*(TG(I-1)-TW)-FL*X*DT*ANU*HTC*TD
513      IF(NI.EQ.1) GO TO 8
515      VP(I)=VP(I-1)+DT*VD/TC1
522      8  TP(I)=TP(I-1)+ANU*HTC*DT*TD/CP

```

C CHECK FOR NEGATIVE ARGUMENT OF SQUARE ROOT

527 ARG=1.-2.*(AK**2-1.)*X*ZG(I)/(AK*YG(I))**2

537 IF(ARG.GT.0.) GO TO 9

541 IF(ARG.LE.0.) VELU=VEL

544 GO TO 2

545 9 VG(I)=VGF(AK, YG(I), X, ZG(I), ARG)

560 DG(I)=DGF(X, VG(I))

564 PG(I)=PGF(X, VG(I), YG(I))

570 TG(I)=TGF(DG(I), RGAS, PG(I))

576 VISK=(AU+BU*TG(I)+CU*TG(I)**2)*.0001

603 REC=DP/VISK

604 TCC=DENP*DP**2/(18.*VISK)

607 RE=VG(I)*DIA*DG(I)/VISK

612 CF=3.051187564E-01*RE**2-2.463091378E-01/4.

617 PNU=.023*RE**8

623 TC=(AT+BT*TG(I)+CT*TG(I)**2)*777.649/3600.

631 HTC=6.*TC*32.174/(DENP*DP**2)

635 FFAC=2*CF*DX/DIA

641 QFAC=32.174*TC*PNU*4*DX/DIA**2

647 IF(NI.EQ.1) VP(I)=VG(I)

C SET INDICATOR IF PARTICLE VELOCITY EXCEEDS GAS VELOCITY

653 IF(VP(I).GT.VG(I)) NI=1

657 10 CONTINUE

662 VC=SQRT(1.4*32.174*PGAS*TG(NUM))*.99

667 IF(VG(NUM).GT.VC) GO TO 11

674 IF(ABS(PG(NUM)-PREF).LE.PRED) GO TO 11

700 IF(PG(NUM).LT.PREF) VELU=VEL

704 IF(PG(NUM).GT.PREF) VELL=VEL

711 GO TO 2

712 11 CONTINUE

712 QSTP=VG(NUM)*AREA*DG(NUM)/.075

C CONVERT OUTPUT TO INPUT UNITS

716 DO 12 J=1, NUM

726 PG(J)=PG(J)/144.-14.696

730 TG(J)=TG(J)-460.

731 TP(J)=TP(J)-460.

732 12 CONTINUE

733 PRINT 50, VG(NUM), VP(NUM), QSTP, RE, TG(NUM), TP(NUM), DG(NUM), PG(NUM)

764 13 CONTINUE

766 14 CONTINUE

770 15 CONTINUE

1 FORMAT(1H1)

20 FORMAT(7F10.3)

25 FORMAT(2F10.3)

30 FORMAT(2X, *PARTICLE DIAMETER*, F10.3, *(MICRONS)*/2X, *INITIAL PARTIC
1LE VELOCITY*, F10.3, *(FT/SEC)*/2X, *TUBE DIAMETER*, F10.3, *(INCHES)*/
22X, *LOAD FACTOR*, F10.3//)

40 FORMAT(2X, *DIFFERENTIAL PRESSURE*, F10.5, *(PSI)*/2X, *GAS VELOCITY*
1, 5X, *PARTICLE VELOCITY*, 8X, *FLOW RATE*, 9X, *FLOW*, 11X, *GAS TEMP*, 7X
2, *PARTICLE TEMP*, 7X, *DENSITY*/4X, *(FT/SEC)*, 11X, *(FT/SEC)*, 11X, *(C
3U-FT/SEC)*, 5X, *REYNOLDS NR.*, 5X, *(FAHRENHEIT)*, 5X, *(FAHRENHEIT)*,
46X, *(LBM/CU-FT)*///)

50 FORMAT(3X, F9.4, 10X, F9.4, 13X, F6.4, 11X, F6.0, 11X, F8.3, 9X, F8.3, 11X, F5.
14/2X, F10.7//)

772 END

```

CROWE6
PROGRAM CROWE6(INPUT,OUTPUT)
C SILICON CARBIDE PARTICLES-280 MICRONS,+60-48,W/LOADING VARIATIONS
  DIMENSION VG(400),DG(400),PG(400),YG(400),ZG(400),TG(400),
  IVP(400),TP(400)
C STATEMENT FUNCTIONS
  VGF(AK,Y,X,Z,ARG)=(AK*Y)/((AK+1.)*X)*(1.-SQRT(ARG))
  DGF(X,VEL)=X/VEL
  PGF(X,VEL,Y)=Y-X*VEL
  TGF(DEN,RGAS,PRE)=PRE/(DEN*RGAS)
  PRINT 1
C COEFFICIENTS FOR INTERPOLATING POLYNOMIAL TO DETERMINE VISK=VISK(R)
  FOR AIR.
51 AU=3.613800798E-02
52 BU=1.75335507E-04
54 CU=-2.175980811E-08
C COEFFICIENTS FOR INTERPOLATING POLYNOMIAL TO DETERMINE TC=TC(R)
  FOR AIR.
55 AT=1.257804164E-03
57 BT=2.784865154E-05
60 CT=-3.813387944E-09
C NUMBER OF STATIONS PER LENGTH OF TUBE
62 NUM=400
C GAS CONSTANTS
63 AK=1.4
64 RGAS=287.
C INPUT DO LOOP
66 DO 15 M=1,8
70 READ 20,DPRE,DDL,TGASC,TWC,DPM,DIACM,FL
111 READ 25,DENP,CCP
121 CPE=CCP
122 TGAS=TGASC+273.
124 VP(I)=1.52
126 PRINT 30,DPM,VP(1),DIACM,FL
143 DIA=DIACM/100.
145 AREA=3.14159*DIA**2/4.
C DIFFERENTIAL PRESSURE DO LOOP
150 DO 14 K=1,1
151 DIFP=DPRE*K
152 DIF=DIFP
154 PRINT 40,DIF
C TUBE LENGTH DO LOOP
161 DO 13 L=1,1
163 DL=DDL*L/100.
C FIND GAS VELOCITY TO PRODUCE DESIRED PRESSURE DROP
165 PRED=DIFP/100.
167 PREF=101325.981
170 PRE=PREF+DIFP
171 VELL=0.
172 DEN=PRE/(RGAS*TGAS)
175 VELU=SQRT(1.4*RGAS*TGAS)
202 2 VEL=(VELL+VELU)/2.
204 TR=TGAS*9./5.
206 VISK=1.48R2*(AU+BU*TR+CU*TR**2)*.0001
214 RE=VEL*DIA*DEN/VISK
217 CF=3.051187564E-01*RE**-2.463091378E-01/4.
223 PNU=.023*RE**.8

```

```

CROWE6
227      X=DEN*VEL
231      Y=PRE+X*VEL
233      Z=X*(VEL**2/2.+AK*PRE/((AK-1.)*DEN))
C      CHECK FOR NEGATIVE ARGUMENT OF SQUARE ROOT
242      ARG=1.-2.*(AK**2-1.)*X*Z/(AK*Y)**2
250      IF(ARG.GT.0.) GO TO 3
253      IF(ARG.LE.0.) VELU=VEL
256      GO TO 2
257      3 VEL=VGF(AK,Y,X,Z,ARG)
267      DEN=DGF(X,VEL)
271      PRE=PGF(X,VEL,Y)
274      TGAS=TGF(DEN,RGAS,PRE)
300      TC=1.7296*(AT+BT*TR+CT*TR**2)*777.649/3600.
306      TW=TWC+273.
C      ADD PARAMETERS FOR GAS-PARTICLE FLOW
310      DP=DPM/1.E+06
312      REC=DP/VISK
314      TCC=DENP*DP**2/(18.*VISK)
317      HTC=6.*TC/(DENP*DP**2)
322      NI=0
322      DX=DL/FLOAT(NUM-1)
325      FFAC=2*CF*DX/DIA
331      QFAC=TC*PNU*4*DX/DIA**2
335      TP(I)=296.9
337      VG(1)=VEL
340      DG(I)=DEN
342      PG(1)=PRE
343      YG(1)=Y
345      ZG(1)=Z
346      TG(1)=TGAS
C      INCREMENTING DO LOOP
350      DO 10 I=2,NUM
352      DT=DX/VP(I-1)
354      TD=TG(I-1)-TP(I-1)
356      IF(NI.EQ.1) GO TO 6
360      VD=VG(I-1)-VP(I-1)
362      IF(NI.EQ.0) GO TO 4
363      GO TO 6
C      MACH NUMBER EFFECTS
363      4 XM=ABS(VD/(SQRT(1.4*RGAS*TG(I-1))))
372      C=1.65+.65*TANH(2.*ALOG(XM))+.425*EXP(-2.5*(ALOG(XM/1.4))**2)
413      REP=REC*DG(I-1)*ABS(VD)
417      IF(REP.LE.200.) GO TO 5
422      IF(REP.LE.2500.) DF=(21.9416*REP**+.718+.324)*REP*C/24.
435      IF(REP.GT.2500.) DF=.4*REP*C/24.
443      GO TO 7
444      5 DF=(1.+.15*REP**+.687)*C
453      GO TO 7
453      6 VD=0.
454      DF=1.
457      7 TC1=TCC/DF
461      ANU=2.+.37*REP**+.6
467      YG(I)=YG(I-1)-FFAC*DG(I-1)*VG(I-1)**2-FL*X*DT*VD/TC1
477      ZG(I)=ZG(I-1)-QFAC*(TG(I-1)-TW)-FL*X*DT*ANU*HTC*TD
510      IF(NI.EQ.1) GO TO 8
512      VP(I)=VP(I-1)+DT*VD/TC1

```


CROWE6

-86-

```

517      8 TP(I)=TP(I-1)+ANU*HTC*DT*ID/CP
      C CHECK FOR NEGATIVE ARGUMENT OF SQUARE ROOT
524      ARG=1.-2.*(AK**2-1.)*X*ZG(I)/(AK*YG(I))**2
534      IF(ARG.GT.0.) GO TO 9
536      IF(ARG.LE.0.) VELU=VEL
541      GO TO 2
542      9 VG(I)=VGF(AK,YG(I),X,ZG(I),ARG)
555      DG(I)=DGF(X,VG(I))
561      PG(I)=PGF(X,VG(I),YG(I))
565      TG(I)=TGF(DG(I),RGAS,PG(I))
573      TR=TG(I)*9./5.
574      VISK=1.48R2*(AU+BU*TR+CU*TR**2)*.0001
602      REC=DP/VISK
603      TCC=DENP*DP**2/(18.*VISK)
606      RE=VG(I)*DIA*DG(I)/VISK
611      CF=3.051187564E-01*RE**-2.463091378E-01/4.
616      PNU=.023*RE**.8
622      TC=1.7296*(AT+BT*TR+CT*TR**2)*777.649/3600.
630      HTC=6.*TC/(DENP*DP**2)
634      FFAC=2*CF*DX/DIA
640      QFAC=TC*PNU*4*DX/DIA**2
645      IF(NI.EQ.1) VP(I)=VG(I)
      C SET INDICATOR IF PARTICLE VELOCITY EXCEEDS GAS VELOCITY
651      IF(VP(I).GT.VG(I)) NI=1
655      10 CONTINUE
660      VC=SQRT(1.4*RGAS*TG(NUM))*.99
665      IF(VG(NUM).GT.VC) GO TO 11
672      IF(ABS(PG(NUM)-PREF).LE.PRED) GO TO 11
676      IF(PG(NUM).LT.PREF) VELU=VEL
702      IF(PG(NUM).GT.PREF) VELL=VEL
707      GO TO 2
710      11 CONTINUE
710      QSTP=VG(NUM)*AREA*DG(NUM)/1.2
      C CONVERT OUTPUT TO INPUT UNITS
714      DO 12 J=1,NUM
722      TG(J)=TG(J)-273.
723      TP(J)=TP(J)-273.
724      12 CONTINUE
725      PRINT 50, VG(NUM), VP(NUM), QSTP, RE, TG(NUM), TP(NUM), DG(NUM), PG(NUM)
757      13 CONTINUE
761      14 CONTINUE
763      15 CONTINUE
          1 FORMAT(1H1)
          20 FORMAT(7F10.3)
          25 FOPMAT(2F10.3)
          30 FOMAT(2X,*PARTICLE DIAMETER*,F10.3,*(MICRONS)*/2X,*INITIAL PARTIC
          1LE VELOCITY*,F10.3,*(M/SEC)*/2X,*TUBE DIAMETER*,F10.3,*(CM)*/
          22X,*LOAD FACTOR*,F10.3//)
          40 FOMAT(2X,*DIFFENENTIAL PRESSURE*,F12.3,*(N/SQ-M)*///2X,*GAS VELOC
          ITY*,5X,*PARTICLE VELOCITY*,8X,*FLOW RATE*,9X,*FLOW*,11X,*GAS TEMP*
          2,7X,*PARTICLE TEMP*,7X,*DENSITY*/5X,*(M/SEC)*,12X,*(M/SEC)*,12X,*(
          3CU-M/SEC)*,5X,*REYNOLDS NR.*,5X,*(CENTIGRADE)*,5X,*(CENTIGRADE)*,7
          4X,*(KG/CU-M)*///)
          50 FOMAT(3X,F9.4,10X,F9.4,13X,F6.4,11X,F6.0,11X,F8.3,9X,F8.3,10X,F6.
          14/2X,F8.3/)
765      END

```

This report was done with support from the United States Energy Research and Development Administration. Any conclusions or opinions expressed in this report represent solely those of the author(s) and not necessarily those of The Regents of the University of California, the Lawrence Berkeley Laboratory or the United States Energy Research and Development Administration.